R-7998

FINAL REPORT

CHAMBER TECHNOLOGY FOR SPACE STORABLE PROPELLANTS

Prepared for

NATIONAL AERONAUTICS AND SPACE ADMINISTRATION

Contract NAS7-304

September 1969

ROCKETDYNE
A Division of North American Rockwell
6633 Canoga Avenue, Canoga Park, California

ACKNOWLEDGMENTS

The accomplishments described in this report were conducted by the Reasearch Division of Rocketdyne. Contributors to the effort are too numerous to mention here. Acknowledgments were extended to individuals in each of the four interim reports.

FOREWORD

This report has been prepared in compliance with NASA Contract NAS7-304 and fulfills the contract requirements for Chamber Technology for Space Storable Propellants. The technical effort reported herein was conducted during the period from June 1964 through September 1969 by the Rocketdyne Research Division.

ABSTRACT

A 5-year applied research program has been conducted to generate chamber technology for several space storable propellant combinations featuring oxygen difluoride (OF_2) oxidizer. The fuels evaluated for combination with OF_2 were monomethylhydrazine (MMH), butene-1 (C_4H_8) and diborane (B_2H_6). Extensive design criteria were developed for OF_2/MMH; performance and heat transfer criteria were developed for OF_2/B_2H_6 and OF_2/C_4H_8.

A full analysis technique was developed for rational selection of optimum fuels for combination with OF_2. Selection of the candidate fuels was based on performance, operational aspects, and compatibility for thrust chamber cooling.

Areas of investigation included injector performance, performance demonstration under simulated altitude conditions for OF_2/MMH, and throttling characteristics for all of the propellant combinations.

Complete assessment of heat transfer characteristics were conducted for each propellant system. Design criteria were generated for either regenerative or ablative cooling with OF_2/MMH. Passive cooling technology was also developed for OF_2/B_2H_6; however, the OF_2/C_4H_8 studies were limited to heat transfer characterization.

CONTENTS

ILLUSTRATIONS

TABLES

INTRODUCTION AND SUMMARY

Chamber Technology for Space Storable Propellants has been a 5-year analytical and experimental program directed to the systematic generation of design criteria for selected space storable fuels in combination with oxygen difluoride (OF_2). Three general types of fuels were considered, from which one specific fuel of each type was selected as best representing their respective chemical families. The fuel types considered were the amines (hydrazines), the light hydrocarbons, and the borane group. Of the amines, monomethylhydrazine (MMH) was selected as the best possible fuel for combination with OF_2, based on performance and payload, operational aspects, and chamber cooling considerations. By the same general criteria, butene-1 (C_4H_8) was considered the optimum choice of the light hydrocarbons (LPG). The third fuel, diborane (B_2H_6) was selected as the most attractive of the high-energy borane group primarily because of its demonstrated high performance characteristics. It was not selected from analytical considerations, as was the case with MMH and C_4H_8.

To summarize the total scope of work conducted during this program, it is helpful to refer to the chronological program logic structure shown in Fig. 1 . At the outset of the program in June of 1964, only two technical tasks were considered for immediate effort.

Task I was to consider several candidate amine fuels, including their derivatives and blends, and to rationally select a single optimum fuel for combination with oxygen difluoride (OF_2) and subsequent experimental evaluation. To arrive at a logical selection of the best fuel, three basic evalution criteria were established so that the rating of each candidate fuel could be accomplished in a quantitative manner. These criteria were performance and payload, operational aspects, and chamber cooling compatibility. The weightings assigned to these general criteria, and also to individual detail criteria within these broad rating areas were somewhat arbitrary in that they necessarily reflected judgement on the importance of each category.

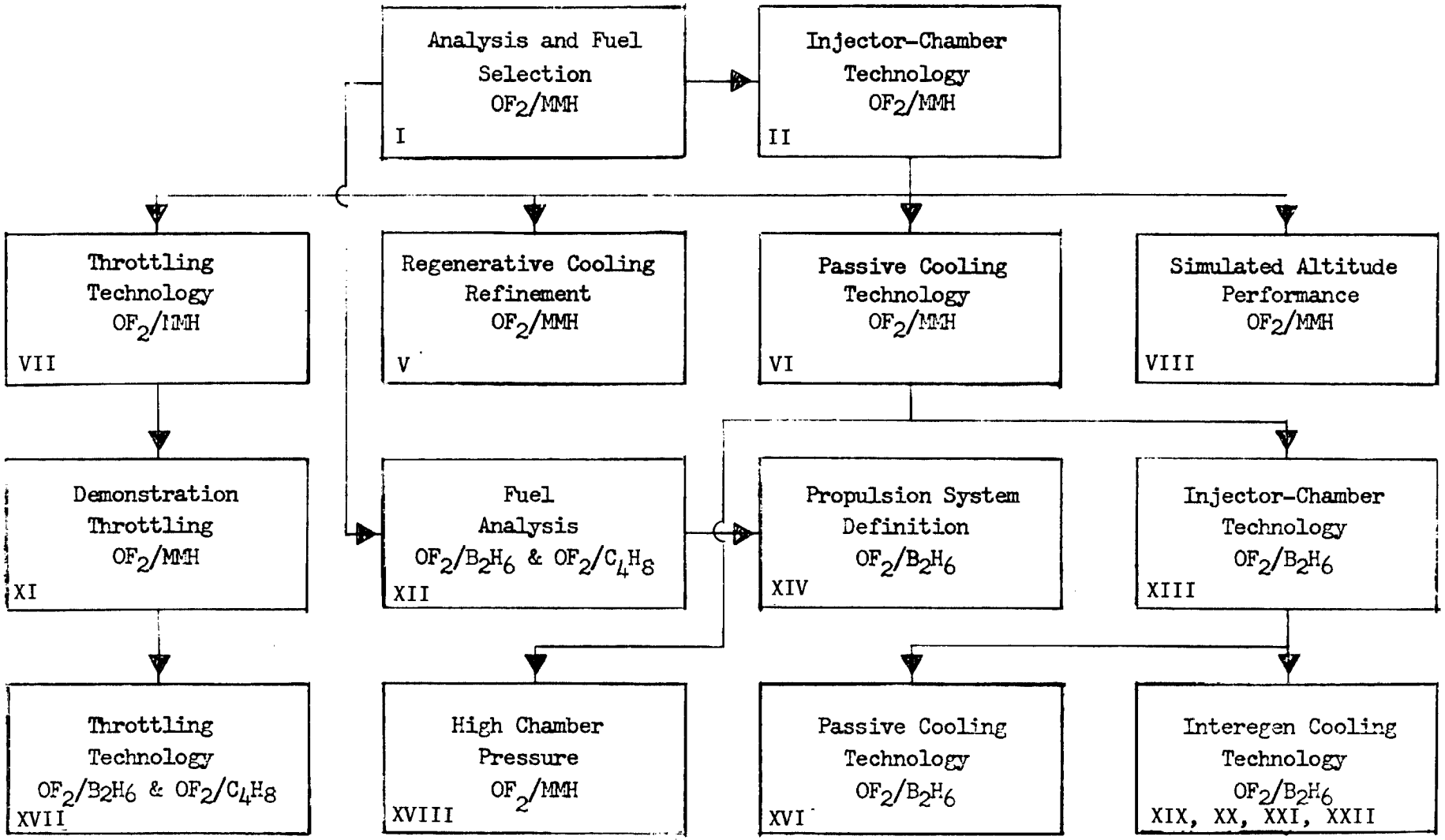

Figure 1. Chamber Technology for Space Storable Propellants (NAS7-304)

Based on this analysis, monomethylhydrazine (MMH) was selected as the optimum fuel for subsequent experimental study. In addition to selection of the fuel, design optimization studies were conducted to establish the best chamber pressure and mixture ratio for maximum payload. A chamber pressure of 100 psia and mixture ratio of 2.0 were selected as best suited for maximum exploitation of this propellant combination.

R-6028-1, Chamber Technology for Space Storable Propellants, Interim Report, Vol. I, Rocketdyne, a Division of North American Aviation, Inc., Canoga Park, California, September 1965, CONFIDENTIAL. *

Task II was conducted to experimentally generate design criteria for the selected OF_2/MMH propellant combination. The majority of all experimental work was conducted with FLOX (70 percent fluorine-30 percent oxygen) as a simulant for OF_2. The FLOX substitute was experimentally verified as an excellent simulant for OF_2 from the standpoint of performance and heat transfer.

A self-impinging doublet injector was selected as the best of three candidate injectors for combined high performance and uniform heat transfer characteristics. Initial experiments were conducted with a composite thrust chamber consisting of an ablatively cooled combustion chamber, a regeneratively cooled throat insert, and an ablatively cooled expansion skirt. An attractive alternate to the regeneratively cooled throat was a monolithic graphite throat insert.

A single self-impinging doublet injector of nickel was fired for an accumulated duration of over 4500 seconds without degradation of either performance or structural integrity. A stainless-steel regeneratively cooled throat was fired for durations up to 600 seconds at design conditions, although

*The referenced report covers the previously described program technical effect in detail. Succeeding work is described more fully in the references appropriately noted in the text.

evidence indicated potential overheating problems near the start of convergence. Other tests were conducted with thrust chambers having a hard graphite throat insert for total durations up to 1700 seconds with only minimum throat erosion.

R-6068-2, Chamber Technology for Space Storable Propellants, Interim Report, Vol. II, Rocketdyne, a Division of North American Aviation, Inc., Canoga Park, California, October 1965.

Based on the encouraging results of these preliminary studies, a program extension, consisting of four technical tasks, was undertaken to extend and advance design technology for these propellants. The first task was to undertake design refinement of the regeneratively cooled throat section to provide a more reliable margin of operation. An analytical re-evaluation of the prevailing chamber heat load indicated that the convergent portion of the nozzle was receiving a high heat load contribution due to thermal radiation from the hot ablative thrust chamber wall. Nozzle design modifications were made, and subsequent experiments up to 400-seconds duration were conducted to prove the effectiveness of these refinements. Additional tests were conducted to define the practical operating limits for regenerative cooling. Multiple start tests were also conducted to demonstrate its practical capability for actual engine usage.

The second task was the generation of design criteria for an all passively cooled carbon-type chamber. Variations in material and geometric parameters were investigated in tests up to 1000 seconds duration using FLOX and MMH. A final verification test of 80 seconds was conducted with the prime OF_2/MMH propellant combination to verify the validity of these design principles.

In the third task, design technology was derived for eventual design of a 10:1 throttling injector using the dual manifold technique for combined area-pressure throttling. An experimental correlation was developed to relate injector design parameters to experimental combustion efficiency. Tests were conducted over a 15-to 150-psia chamber pressure range with measured c* efficiencies ranging from 92 to 97.5 percent.

A fourth task was directed toward evaluation of altitude performance for both OF_2/MMH and FLOX/MMH in a thrust chamber having a 20:1 expansion area ratio. High delivered performance was consistent with preceding sea-level tests. The results of these experiments enabled preliminary design of a lightweight, flight-type thrust chamber configuration which was shown to be directly competitive with conventional tube wall thrust chambers in terms of weight.

R-6561-2, Chamber Technology for Space Storable Propellants, Second Interim Report, Rocketdyne, a Division of North American Aviation, Inc., Canoga Park, California, September 1966.

A subsequent program extension was granted to further extend design criteria to other candidate fuels for use with the OF_2 oxidizer and to refine preceding design information. Additional work was accomplished to design, fabricate, and demonstrate the performance characteristics of a fully throttleable OF_2/MMH injector. The design was based on criteria developed from the preceding exploratory study in which only fixed point performance tests were conducted. A fully throttleable dual manifold injector was fabricated of nickel and demonstrated to be completely and continuously throttleable over a 10:1 thrust range.

Using analytical techniques in the first program task, studies were conducted to select an optimum light hydrocarbon fuel (LPG) for combination with the OF_2 oxidizer. Based on encouraging performance results during an internally sponsored feasibility program, diborane (B_2H_6) was also selected for analytical evaluation. Based on comparison of methane, propane, and butene-1, the latter LPG fuel (C_4H_8) was selected as best representing the LPG type fuels for combination with OF_2. Following selection of C_4H_8 and B_2H_6 as promising candidate space-storable fuels, further analyses were conducted to compare these two fuels with the previously selected MMH fuel. Although a clear-cut selection of the best fuel could not be made, the specific rating areas gave clear indication of fuel characteristics for various applications and in the three basic rating categories. It

was readily apparent that selection of a best fuel would be strongly dependent on definition of a specific mission and application.

Based on the selection of a hypothetical near-term space mission, a preliminary systems analysis was conducted to define a propulsion system to suit this application. The OF_2/B_2H_6 propellant system was determined to best satisfy these requirements.

The highly encouraging outlook for B_2H_6 in combination with OF_2 prompted allocation of a task to determine if design criteria previously developed for OF_2/MMH could be directly applied to the OF_2/B_2H_6 system. Although performance characteristics were amenable to correlation with preceding criteria, heat transfer and chamber compatibility for OF_2/B_2H_6 was significantly more severe than that previously experienced with OF_2/MMH.

The results of these early experiments clearly indicated the need for additional emphasis toward improvement in thrust chamber compatibility for this propellant combination.

R-7073, Chamber Technology for Space Storable Propellants, Third Interim Report, Rocketdyne, a Division of North American Aviation, Inc., Canoga Park, California, May 1967.

A final program extension was conducted to concentrate primarily on defining design requirements for a high-performance, long-duration thrust chamber assembly for the OF_2/B_2H_6 propellant combination. One task was specifically designed to study the OF_2/B_2H_6 propellant system for compatibility with an ablatively cooled thrust chamber. Primary design emphasis was toward manipulation of injector design parameters to maintain high c* performance while simultaneously improving chamber compatibility characteristics. Although completely successful operation was not demonstrated in this task, specific valuable design criteria were developed for eventual attainment of injector-chamber compatibility.

Because of the high technical risk involved in eventual attainment of a suitable ablative thrust chamber assembly, additional tasks were assigned to potential application of the novel Rocketdyne-developed interegen cooling concept to OF_2/B_2H_6. Feasibility studies were conducted and indicated that film cooling with B_2H_6 fuel was entirely possible and that graphite could be used as a thrust chamber material for internal heat conduction to the B_2H_6 liquid film. Supporting experiments were conducted to select a suitable injector design and to attain necessary design information for construction of a final thrust chamber assembly.

Based on the experimental results, an interegen thrust chamber was designed and fabricated for experimental evaluation in long-duration tests. One test, programmed for approximately 300 seconds, was prematurely terminated after 45 seconds because of visual evidence of sudden chamber failure. Posttest analysis indicated chamber structural failure rather than thermal chemical degradation, a characteristic of this propellant combination. Structural analysis indicated that the probable mode of failure was localized overheating and resultant chamber material failure followed by catastrophic rupture of the complete thrust chamber assembly. The results did not conclusively determine the basic feasibility of interegen cooling for the OF_2/B_2H_6 propellants.

A task was also allocated to extension of previously developed OF_2/MMH chamber technology to higher chamber pressures. With some improvement and refinement of the basic self-impinging doublet injector, experiments were conducted to show that completely satisfactory operation could be anticipated at chamber pressures up to 500 psia. A single test conducted with a lightweight, flight-type thrust chamber assembly provided experimental verification of the design criteria for satisfactory applicability to higher chamber pressures.

To complete this program, a final task was conducted to acquire necessary design technology for eventual design and fabrication of fully throttleable OF_2/B_2H_6 and OF_2/C_4H_8 dual-manifold injectors. Additional effort was expended in design of a completely integrated throttle valve assembly for flight-weight application.

R-7985, Chamber Technology for Space Storable Propellants, Fourth Interim Report, Rocketdyne, a Division of North American Rockwell Corporation, Canoga Park, California, September 1969.

FUEL SELECTION

Chamber Technology for Space Storable Propellants has been a 5 year analytical and experimental program directed toward systematic development of design criteria for selected space-storable fuels in combination with oxygen difluoride (OF_2). With identification of oxygen difluoride (OF_2) as a promising space-storable oxidizer, a comprehensive analytical study was undertaken to select appropriate complementary fuel candidates. The fuel types considered best suited for combination with OF_2 were the hydrazines (or amines), light hydrocarbons, and a borane fuel. The fuels considered are listed in Table 1.

Of the amine fuels, monomethylhydrazine (MMH) was selected as the best possible fuel for combination with OF_2 based on performance, operational aspects, and chamber cooling considerations. By the same general criteria, butene-1 (C_4H_8) was considered the optimum choice of the light petroleum gases (LPG). The third fuel, diborane (B_2H_6), was arbitrarily chosen as the most attractive of the high-energy borane group, and, for expedience, was not compared analytically with the other higher boranes. The selection of diborane for experimental study was prompted by early in-house studies in which the high performance potential of OF_2/B_2H_6 was conclusively demonstrated during a brief experimental program.

Three general rating categories were considered as evaluation criteria for the fuel rating. The basic areas of evaluation were performance, operational aspects, and thrust chamber cooling. No attempt was made to develop a generalized overall rating for consolidation of the three basic rating categories. To make an overall evaluation of the numerous fuel candidates, gross assumptions would have to be projected as to specific mission and duty cycle for the space-storable propulsion system. It was apparent from this analysis that no one fuel or fuel class could be rated as optimum for all applications.

When a specific mission objective can be defined for this general class of space-storable propellants, it is probable that the ultimate selection of the specific propellants will not be based on an overall rating, but on

TABLE 1

FUEL CANDIDATES SELECTED

Hydrazine-Ammonia (Derivatives and Blends)

Neat Fuels

Hydrazine: N_2H_4

Monomethylhydrazine (MMH): CH_3HNNH_2

Unsymmetrical Dimethylhydrazine (UDMH): $(CH_3)_2NNH_2$

Ammonia: NH_3

Binary Blends

50-50 (Aerozine 50): N_2H_4-UDMH (50-50)

MHF-3: N_2H_4-MMH (14-86)

MAF-4 (Hydyne, U-DETA): UDMH-DETA* (60-40)

Ternary Blends

MHF-5: N_2H_4-MMH-$N_2H_4.HNO_3$ (26-55-19)

Hydrazoid-P: N_2H_4-MMH-$HClO_4$ (36-41.4-22.6)

BA-1014: N_2H_4-MMH-H_2O (66.7-24.0-9.3)

MAF-1: UDMH-DETA-CH_3CN (40.5-50.5-9.0)

Light Hydrocarbons (LPG)

Methane: CH_4

Propane: C_3H_8

Butene-1: C_4H_8

Boranes

Diborane: B_2H_6

*DETA (diethylene triamine): $\left([NH_2CH_2OH_2]_2NH\right)$

ability to satisfy specific critical requirements. As a general class of fuels, it was necessary to arrive at an overall composite rating for the hydrazine-ammonia and the light hydrocarbon fuels to enable selection of a single best amine and LPG candidate fuel for subsequent experimental evaluation. Although MMH, C_4H_8, and B_2H_6 are compared in the various general rating categories, a composite fuel analysis could not be logically derived.

Payload performance for each candidate fuel was based on potential application to three identifiable contemporary propulsion requirements of the lunar and near-term post-Apollo space missions. Design specifications for these space mission systems were selected to provide specific criteria for realistic evaluation of the candidate fuels. A fourth hypothetical low-thrust mission was arbitrarily included for consideration so that a wider thrust range could be considered. Although more detailed optimization studies were undertaken for the amine fuels, the analysis was generally restricted to fuel selection rather than design optimization. Optimization of engine design parameters would tend to maximize the absolute payload capabilities of each propellant combination; however, relative comparison of the candidate fuels would generally remain unaffected.

Operational aspects for each propellant combination were considered to be a critical parameter for rational selection of an optimum fuel in each general chemical category. Criteria considered in this category include: (1) propulsion system experience, (2) anticipated ease of development, and (3) propellant logistics. Unlike propellant assessment from the standpoint of performance or cooling compatibility, the many areas in operational aspects could be subjective since absolute standards could not be applied. Regardless of the qualitative nature of this propellant rating category, it was considered essential for rational selection of an optimum fuel candidate.

Cooling compatibility as a specific general rating category was considered to be similar to performance and payload assessment since quantitative rating criteria could be generally applied. The selection of a specific optimum fuel in each chemical class was based on suitability for at least

one of the current accepted methods for chamber cooling: regenerative, ablative, and passive. Of equal importance to cooling capability was the thermal-chemical compatibility of each propellant combination with the chamber materials.

PERFORMANCE AND PAYLOAD

Relative performance was based on potential application to several space missions which had design requirements for vehicle size and ideal stage velocity and propellant storage requirements. As shown in Table 2 , the specific space missions considered were those represented by the Apollo service module, Apollo descent stage, Mars excursion module, and arbitrary, unspecified low-thrust (1000 pounds) missions. With these selected propulsion systems, gross weight ranged from 2,000 to 90,000 pounds, ideal stage velocity from approximately 8,000 to 18,000 ft/sec, and thrust range from 1,000 to 30,000 pounds. The arbitrarily selected storage times ranged from "no-storage" up to a duration of 2 years. The comparison between MMH, C_4H_8, and B_2H_6 was made on a no-storage basis.

TABLE 2

VEHICLES FOR PERFORMANCE ANALYSIS

Vehicle	Gross Weight, pounds	Approximate Propellant Weight, pounds	Ideal Change in Stage Velocity, ft/sec	Thrust, pounds
Apollo Service Module	90,000	35,000	8,760	21,500
Apollo Descent Module	28,000	13,500	7,750	10,500
Mars Excursion Module (Ascent)	39,000	29.500	17,100	30,000
Low-Thrust Mission	2,200	1,700	18,000	1,000

To arrive at delivered specific impulse performance, detailed analysis was conducted to determine the thrust chamber losses resulting from aerodynamic drag, divergence, and reaction kinetics. A chamber pressure range of 100 to 1000 psia at their respective optimum OF_2/fuel mixture ratios was considered for each selected fuel. The reference chamber considered in the analysis featured a 60:1 bell nozzle (80 percent) with a circular throat contour having a radius of curvature five times the throat radius. This configuration did not necessarily represent an optimized geometry for the specific propellants considered or for the nominal chamber operating conditions. However, studies during a recent fluorine/hydrogen performance study generally indicated that a large radius of curvature was beneficial for attenuation of kinetics losses. For the analysis, a combustion efficiency, η_{c^*}, of 97.5 percent was assumed as a nominal reference point for evaluation of the candidate fuels in combination with OF_2. Attainment of this efficiency level has since been demonstrated with each of the selected fuels in their respective categories.

Vacuum Specific Impulse

The theoretical propellant characteristics for C_4H_8, MMH, and B_2H_6 in combination with OF_2 are listed in Table 3 . In addition, supplementary data are also tabulated for combinations with optimum FLOX mixtures. Table 3 lists the various propellant combinations considered, its optimum mixture ratio, corresponding combustion temperature, the vacuum specific impulse, bulk specific density, and the density impulse for each combination. Of specific interest, is the wide range of mixture ratios and the corresponding bulk density for each of the propellant combinations. A comparison of both specific and density impulse values for the three propellant combinations is shown in Fig. 2 . For weight limited propulsions systems maximum vacuum specific impulse for OF_2/B_2H_6 is easily superior to either OF_2/C_4H_8 or OF_2/MMH. However, for volume limited applications where bulk density becomes important, the higher relative fuel density for MMH provides a significantly higher density impulse than that for the other two fuel combinations.

TABLE 3

PERFORMANCE CHARACTERISTICS OF CANDIDATE SPACE-STORABLE FUELS IN COMBINATION WITH OF_2 AND WITH OPTIMUM FLOX MIXTURES

Candidate Combination	Optimum Mixture Ratio, o/f	Optimum F_2/O_2 Ratio, percent	Temperature R	Vacuum Impulse, $\frac{lb_f\ sec}{lbm}$	Bulk Density, $\frac{gm}{cm^3}$	Density Impulse*, $\frac{lb_f\ sec\ gm}{lbm\ cm^3}$
OF_2/MMH	2.50		7106	415.4	1.255	521.3
OF_2/C_4H_8	3.85		7707	419.0	1.150	481.9
OF_2/B_2H_6	3.87		7585	445.2	1.007	448.5
FLOX/MMH	2.82	88/12	7644	424.0	1.239	526.0
$FLOX/C_4H_8$	3.85	70/30	7617	412.3	1.084	446.9
$FLOX/B_2H_6$	5.70	81/19	8106	442.7	1.065	471.5

*Shifting Equilibrium: P_c = 100 psia, Expansion Area Ratio (ε) = 60:1

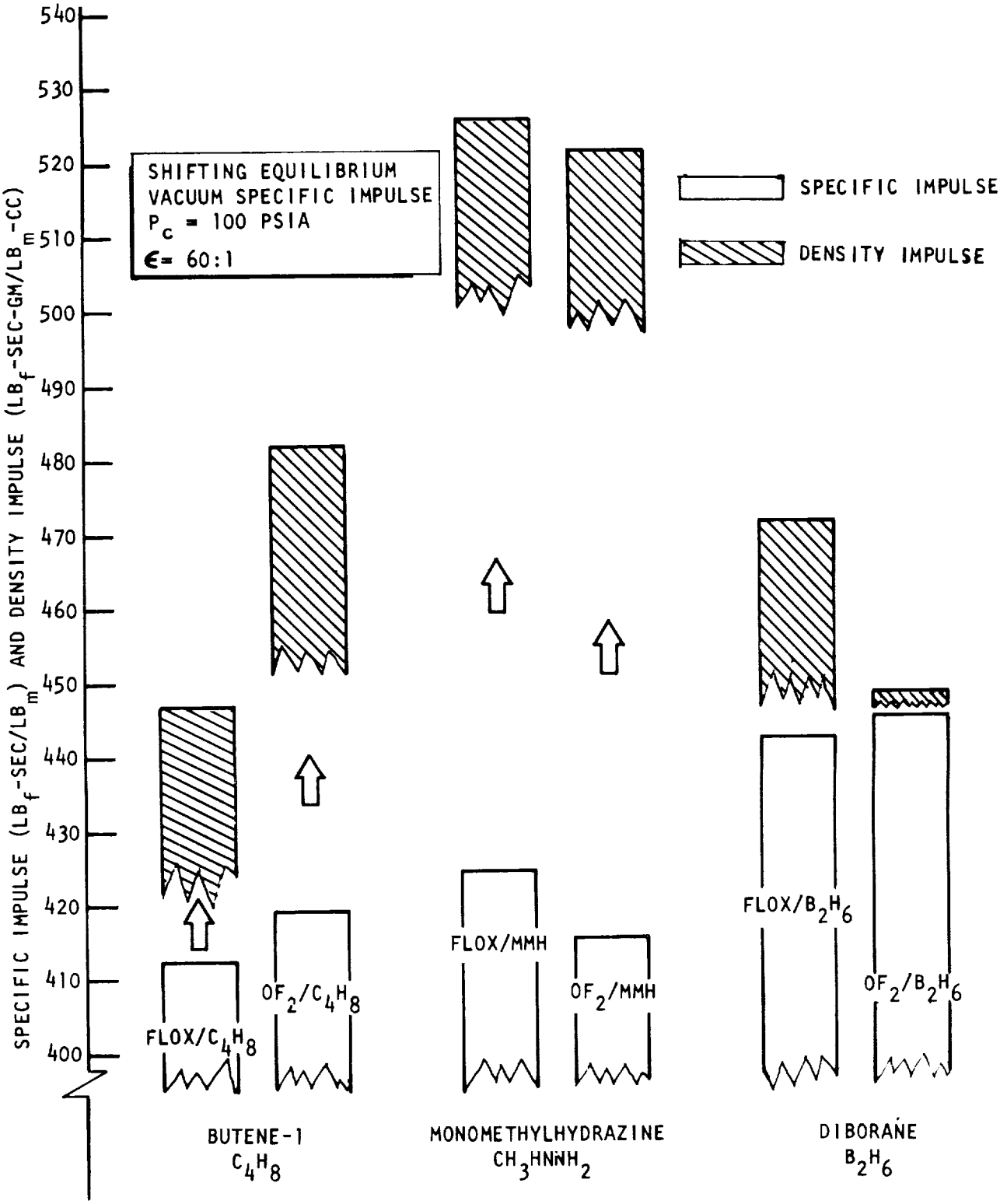

Figure 2. Specific Impulse and Density Impulse for FLOX (Optimum) and OF_2 in Combination With Various Space-Storable Fuels

The one specific drawback to consideration of MMH for space-storable application is its relatively high freezing point and the lack of a common liquidus overlap with either the cryogenic OF_2 or FLOX oxidizer. However, with recent advancement in tank insulation techniques, consideration of OF_2 or FLOX with MMH is not wholly unrealistic. With both external and interface insulation, the OF_2/MMH propellant combination is highly attractive for advanced space-storable propellant combinations. Of course, with either C_4H_8 or B_2H_6, a specific common liquidus range exists with OF_2, and its applicability to near-term space missions is ideally practical.

Butene-1 (C_4H_8) and MMH appear quite similar with respect to maximum attainable performance. There is no clearcut margin of absolute performance superiority for these two propellant combinations.

For this analysis, hypothetical comparison is made between the three candidate fuels on a no-storage basis. This analytical technique tends to bias the final payload and performance rating of the candidate fuels to that having the highest specific impulse and average density. Although various storage time requirements were considered for the more detailed analysis, the simplified approach is demonstrated here to indicate that the real selection of a propellant combination is based on consideration of the deliverable specific impulse from each propellant combination. Allowance for insulation requirements will normally be reflected in a decrement to the deliverable payload in terms of system tank and insulation weights.

Nozzle Geometric Loss. The nozzle geometric loss of a bell nozzle will vary with the propellant combination, chamber pressure, and mixture ratio because of accompanying changes in the combustion gas properties. For this specific study, however, existing geometric loss data for a fluorine/hydrogen system at 100-psia chamber pressure were used for all of the oxygen difluoride/fuel combinations to simplify this analysis. The actual nozzle geometric loss for a given chamber profile is normally derived by a Rocketdyne-developed machine computer program which analyzes variable-property flow fields in the nozzle. The variation of this loss decrement

with the various propellant combinations is not significant (a maximum of 0.5 percent). A geometric loss factor of 1.22 percent was assigned to all three propellant combinations for this analysis.

Drag Loss. The drag analysis was conducted using a computer program which performs a numerical integration of the integral momentum equation for an axisymmetric boundary layer with pressure gradient. The drag loss ($\Delta C_F/C_F$ ideal) for each of the propellant combinations at their respective design mixture ratio and a chamber pressure of 100 psia was computed for a range of chamber pressures from 100 to 700 psia and thrust levels from 1,000 to 30,000 pounds. A characteristic length of 35 inches and a turbulent boundary layer was assumed. As shown in Fig. 3 , the drag loss was found to be relatively insensitive to the specific fuels; the maximum difference was 0.13 percent. This invariance is caused by the similar propellant properties of these bipropellant combinations. The variation of drag loss with chamber pressure is approximately 0.2 percent over the 100-to 700-psia range. The variation of drag loss with thrust is approximately 0.7 percent over the 1,000- to 30,000-pound thrust range being considered.

Reaction Kinetic Loss. The reaction kinetic loss of the nozzle was determined, in part, by performing a stream tube (axisymmetric) kinetic performance analysis. In this method of analysis, the nozzle flow is divided into a large number of stream tubes of equal mass flow, and the Bray criterion is applied to the essentially one-dimensional flow contained in each stream tube. This analysis provides a detailed kinetic evaluation of nonuniform nozzle flow fields. During this study, a stream tube kinetic analysis was performed with OF_2/MMH at a chamber pressure of 100 psia and a mixture ratio of 2.5:1. In addition, a one-dimensional kinetic analysis for the same condition was conducted. This enabled computation of a correction factor (a function of engine thrust) to be applied to one-dimensional data to account for the nozzle flow field nonuniformities. This correction factor was applied to one-dimensional kinetic loss data for the other propellant combinations. As shown in Fig. 4 the OF_2/B_2H_6 propellant system exhibits the lowest losses while the OF_2/C_4H_8 (approximately 2.5 percent at 100 psia chamber pressure) system exhibits the highest losses.

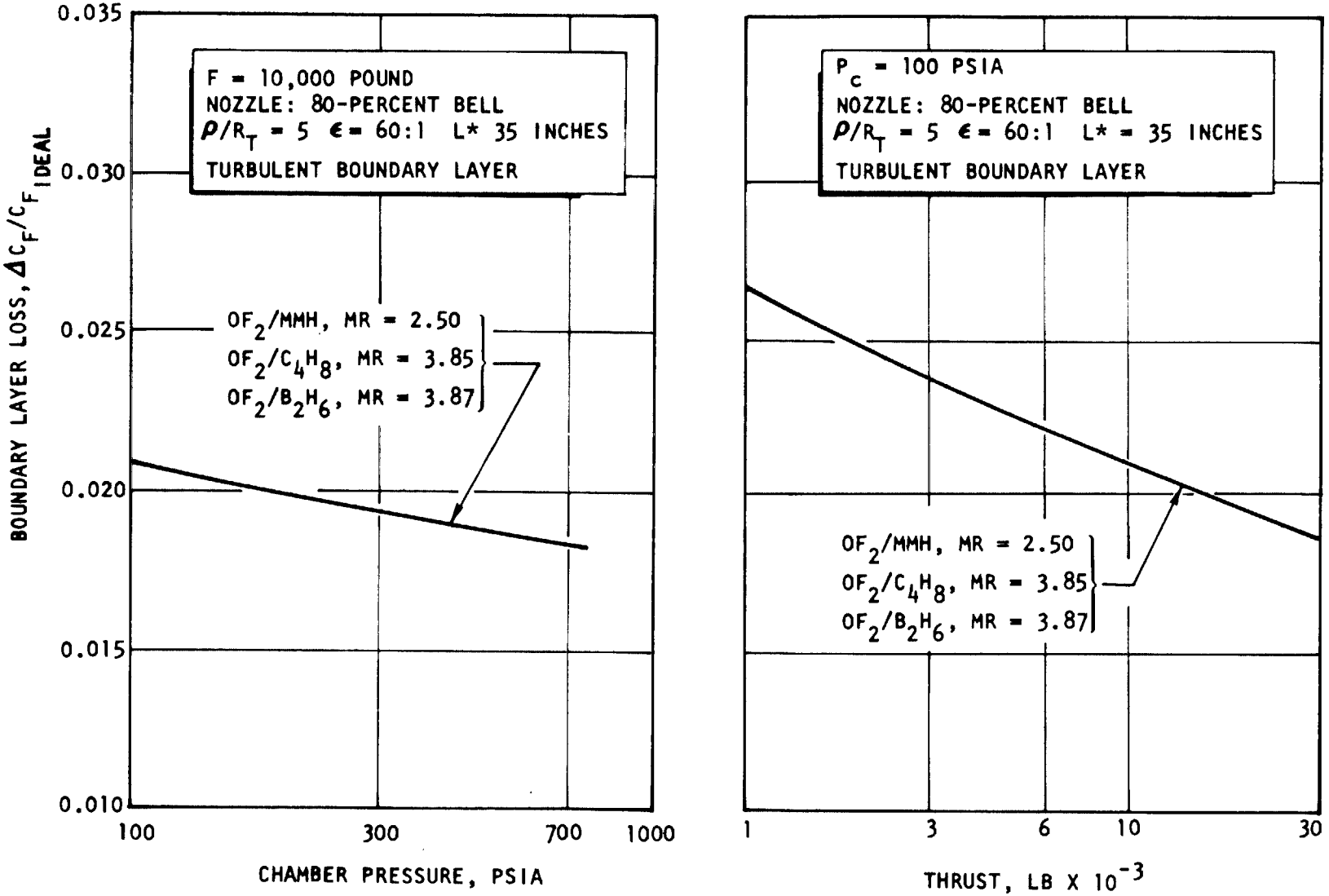

Figure 3. Boundary Layer Loss for Three Candidate Space Storable Propellant Systems

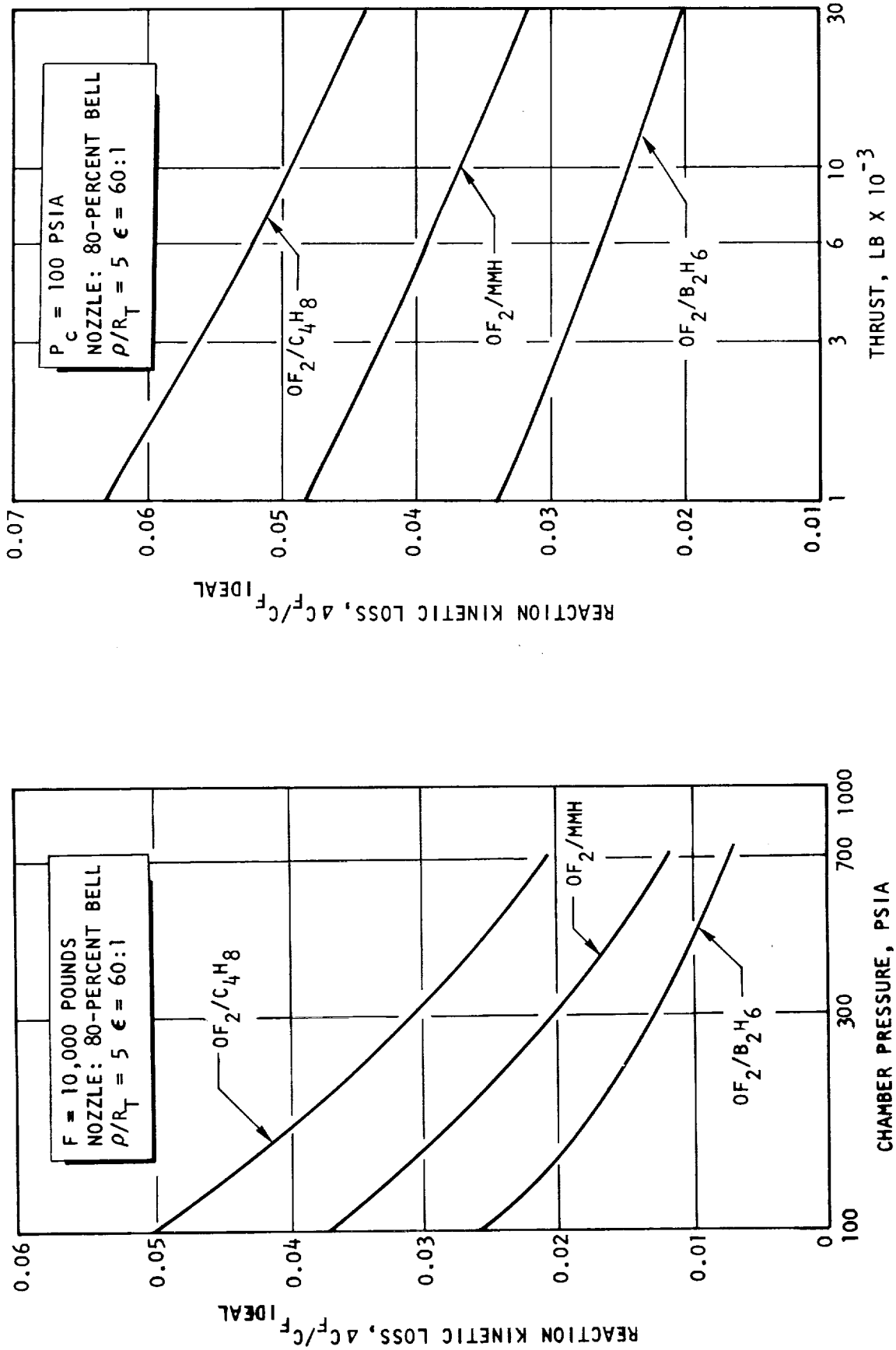

Figure 4. Reaction Kinetic Loss for Three Candidate Space Storable Propellant Systems

By combination of the three previously established nozzle performance decrements with the reference c* efficiency (97.5 percent), a measure of the maximum deliverable specific impulse may be determined for each of the propellant combinations considered. The deliverable vacuum specific impulse for the three propellant combinations is shown as a function of thrust in Fig. 5 . The functional relationship of specific impulse to thrust derives from consideration of the two thrust-dependent nozzle loss decrements. The superiority of OF_2/B_2H_6 with respect to the other two candidate systems is again evident; however, a relative performance shift between OF_2/MMH and OF_2/C_4H_8 is evident (when compared to Table 3). The slight relative superiority of MMH in comparison to C_4H_8 occurs primarily because of a higher kinetic loss encountered with the LPG systems.

Payload

The propellant combinations were evaluated at each of the selected mission conditions to provide a comparison of no-storage payload capability. The values obtained for each propellant system are presented in Table 4 ; the combination OF_2/B_2H_6 is seen to be clearly superior to the other propellant combinations, while OF_2/MMH has an average payload capability approximately 10 percent higher than that for OF_2/C_4H_8.

The effect of prolonged space storage upon vehicle propellants can degrade performance in two ways: (1) because of requirements for venting of propellants, or (2) because of the inert weight of thermal protection systems. Selection of propellants for extended space missions must include consideration of the degradation of performance cause by the propellant storage effects. Any such study requires a mission duty cycle, definition of required storage duration, and detailed vehicle design.

Instead of a detailed storability study, a preliminary evaluation of storage may be made on the basis of allowable propellant temperature range. Such a study was performed for the candidate fuels assuming random vehicle orientation.

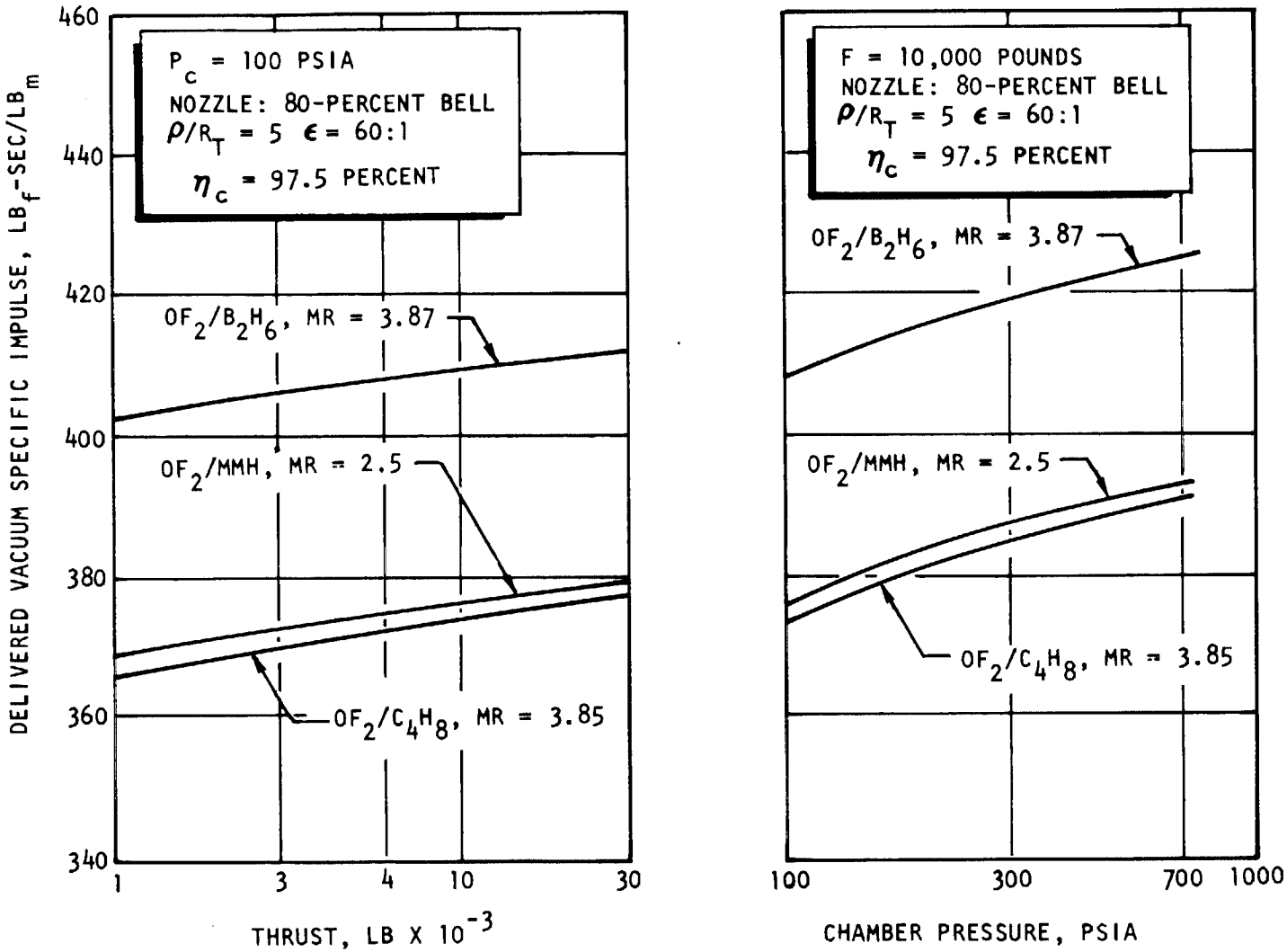

Figure 5. Delivered Vacuum Specific Impulse

TABLE 4

PAYLOAD COMPARISON

(No Space Storage)

Propellant	Apollo Service Module Payload, pounds	Apollo Descent Stage Payload, pounds	Mars Excursion Module Payload, pounds	Low-Thrust Mission* Payload, pounds
OF_2/MMH	34,800	13,090	5530	291
OF_2/C_4H_8	34,000	12,840	5380	258
OF_2/B_2H_6	36,900	12,780	6440	314

*Thrust = 1000 pounds; gross weight = 2200 pounds; change in stage velocity = 18,000 ft/sec

The allowable propellant temperature range is specified by the propellant freezing point and the maximum temperature that can be tolerated before venting becomes necessary. The maximum allowable temperature can be set by either the maximum vapor pressure or the maximum liquid expansion. In general, the maximum allowable vapor pressure for pump-fed systems can be used to set the temperature limit, and the liquid expansion corresponding to the vapor pressure can be accommodated by an ullage volume. For pressure-fed systems, the ullage corresponding to the allowable vapor pressure may be so large that the performance loss caused by inert weight associated with the large tank volume may be greater than the performance loss associated with propellant venting at lower vapor pressures.

An extended interplanetary-type mission requiring multiple engine restarts and long coast periods was assumed for this analysis. The selected space storable propellants, OF_2/B_2H_6, are particularly suited for this type of mission. For many advance-long-range missions, the space environment complements the normal liquid range of both propellants, thus eliminating or

minimizing the need for propellant tank external and intertank insulation. The OF_2/C_4H_8 propellant system also has a specific common liquidus range; however, OF_2/MMH does not; the latter propellant would necessarily require insulation in one or both propellant tanks.

A range of expected environmental temperatures at assumed vehicle absorptivity to emissivity ratios are shown for several advanced missions in Fig. 6 , together with the normal tank liquid ranges for the OF_2 oxidizer and the three space-storable fuels being considered. Where possible, minimum vehicle temperatures were maintained above the propellant freezing points. However, material limitations made this impossible for the deep space (Pluto) mission. Oxygen difluoride would require thermal protection for all missions except the deep-space mission.

OPERATIONAL ASPECTS

Each propellant combination was assessed on other important selection criteria in addition to the prime performance and thrust chamber cooling considerations. An arbitrary assignment of: (1) experience, (2) ease of system development, and (3) propellant logistics permits a more complete evaluation of each candidate propellant combination. This type of analysis was originally employed at the outset of this program to select the best amine-type fuel for combination with oxygen difluoride.

Experience

Industry-wide experience in the areas of ignition tests, research thrust chamber tests, thrust chamber and feed system development, and engine system development indicate the background effort necessary to develop a complete engine system. Some preliminary effort has been accomplished in all of these areas; however, specific engine system development has not been completed for any of the propellant combinations being considered. In general, all candidate propellant systems are quite similar in this category.

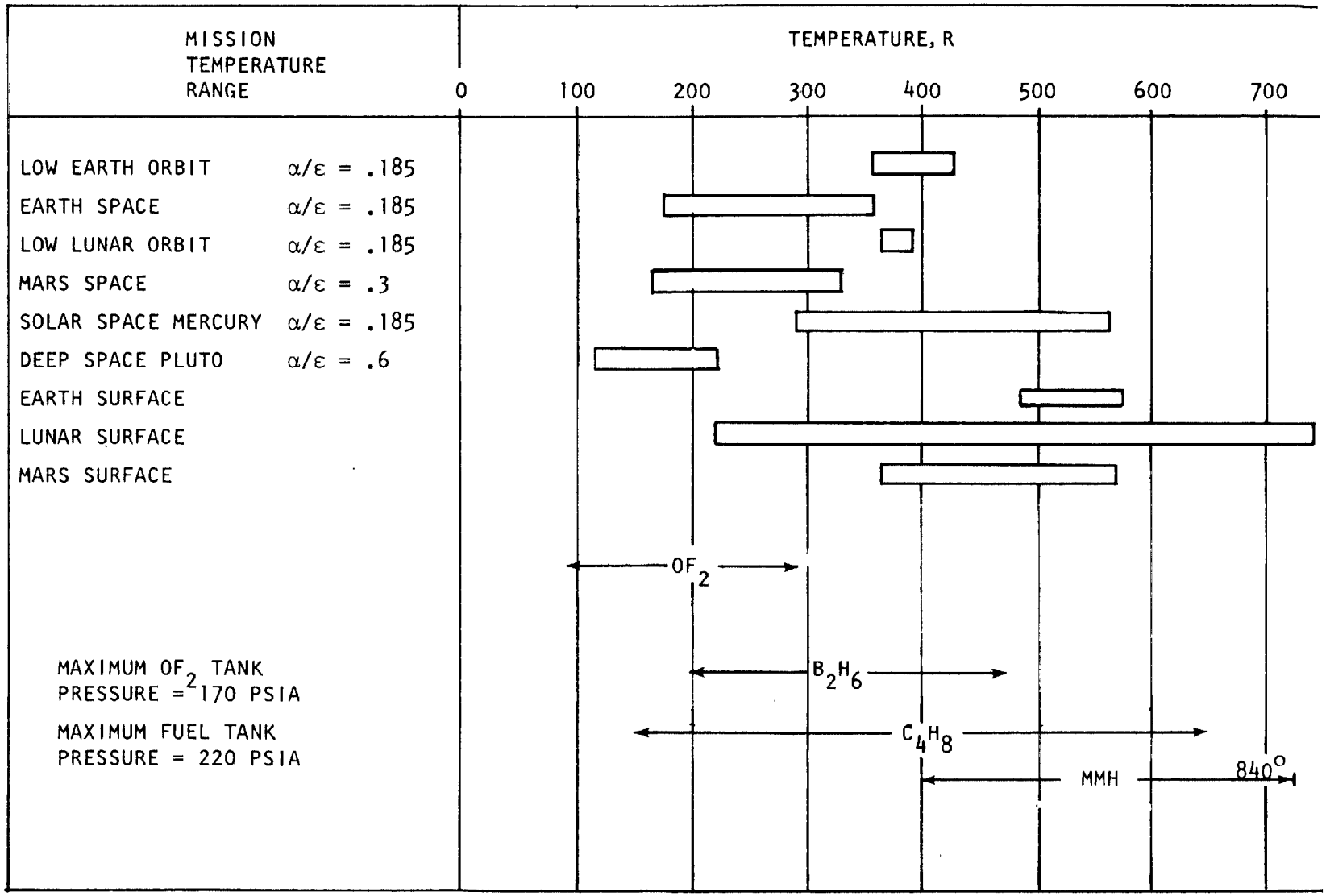

Figure 6. Maximum Allowable Temperature Ranges for Unvented Storage for Oxygen Difluoride and Candidate Fuels and Expected Space Temperature Environment

System Development

The ease of system development for each propellant combination was based on system simplicity and system sensitivity. The factors affecting system simplicity were: (1) propellant combination hypergolicity, (2) purge requirements, (3) hardware chilldown requirements, and (4) dual pressurization system requirements.

The hypergolicity of the OF_2/MMH and OF_2/B_2H_6 propellant combinations simplifies the overall system design by eliminating the requirements for a separate ignition source. The C_4H_8 light hydrocarbon is nonhypergolic with OF_2 and would require an auxiliary ignition device. A purge system would normally be required for all of the systems considered.

Hardware chilldown would generally be required for all of the propellant systems considered to enable smooth, predictable, and stable thrust buildup. Dual pressurization systems, requiring a different pressurant for the oxidizer and the fuel, increase the complexity of the system design. Because helium is compatible with all of the propellants considered, this requirement arises only when system flow characteristics dictate a wide variance, in propellant tank pressure.

Propellant sensitivity indicates the relative variations in propulsion system operation caused by the variation of propellant density or viscosity with temperature. Propellants with low normal boiling points may gain heat during storage, thereby decreasing in density and increasing in volume. Large decreases in density may lead to large ullage requirements which affect the stage tank weights. Large decreases or increases in density affect the propellant utilization system in controlling the mixture ratio. Propellants with relatively high normal boiling points may lose heat, thereby increasing density and viscosity. Large increases in viscosity may produce excessive pressure losses in the system.

Propellant combinations having a common liquidus temperature range between the fuel and oxidizer are desirable because a storage temperature can be achieved to ensure that density and viscosity changes are negligible. Of the three propellant systems, only OF_2/MMH does not have a common liquidus temperature range, thus indicating a definite need for inter-tank insulation in addition to normal thermal protection requirements.

Propellant Logistics

A comparison of logistics indicates the relative ease with which a propellant system development program can be conducted using a given propellant combination. Factors considered were (1) availability, and (2) handling.

Based on current commercial production capability, all of the propellants considered are available in quantities sufficient for a system development program.

Propellant handling indicates the relative difficulty in system development and operation because of propellant toxicity and compatibility. Highly toxic propellants create problems during transport, storage, and testing. Launch pad operations will also require special care and the possibility of low-altitude abort must be considered.

Because of the high toxicity and limited materials compatibility of oxygen difluoride, the handling characteristics of all of the propellant combinations would be similar, with the possible exception of OF_2/B_2H_6 by reason of the additional explosive and toxicity hazards attributed to the diborane fuel.

In summary, the overall operational aspects of each propellant combination are quite similar. The hypergolicity of OF_2/MMH and OF_2/B_2H_6 is a favorable factor in terms of system simplicity, while sensitivity to temperature detracts somewhat from the attributes of OF_2/MMH.

THRUST CHAMBER COOLING

The propellant system capabilities for regenerative, ablative, and radiative cooling were considered for each system.

Regenerative Cooling

There are three basic physical phenomena to be considered for a regeneratively cooled system: (1) heat flux incident on the thrust chamber wall, (2) heat capacity of the coolant, and (3) coolant jacket pressure loss.

To avoid the specific design of thrust chambers for each propellant combination, a simple parametric approach was used. The pertinent equations for a more detailed analysis were employed, and modified by eliminating those parameters which were equal or nearly equal for each propellant system. The results of this simplified analysis were then used as a relative comparison factor.

The relative heat flux (Q/A) and the coolant heat capacity (Q_T/F) were calculated, and a ratio was derived to arrive at a single parametric quotient describing its relative cooling capability. The rating ratio $(Q/A)/(Q_T/F)$ is listed in Table 5 for each propellant combination. Consideration of coolant jacket pressure drop provides an additional factor for assessment of the regenerative cooling capability for each propellant combination. The pressure drop factor accounts for the incident heat flux and the liquid coolant transport properties. The regenerative cooling capability of B_2H_6 did not appear as favorable as ablative for low-chamber-pressure application. The OF_2/MMH system would be favored over OF_2/C_4H_8 because of a much more favorable coolant jacket pressure drop.

Ablative Cooling

The basic factor to be considered for ablative cooling is the compatibility of the chamber material to the exhaust gases and to the resulting gross char rate within the ablative material. Surface erosion is generally caused

TABLE 5

THRUST CHAMBER COOLING COMPARISON

Propellant	Mixture Ratio, o/f	$\frac{Q/A}{Q_T/F}$	ΔP Factor	Combustion Temperature, R	Water Content in Exhaust at Throat, gm mole/100 gm
OF_2/C_4H_8	3.85	343	0.067	7582	0.00
OF_2/B_2H_6	3.87	585	0.169	7533	0.029
OF_2/MMH	2.50	103	0.009	6970	0.133

by either chemical or mechanical erosion. Chemical erosion is accelerated at high temperatures, while reactive species in the exhaust gases also contribute to surface chemical reaction of carbon-base ablative materials. With respect to combustion temperature, the OF_2/C_4H_8 and OF_2/B_2H_6 appear less attractive than the OF_2/MMH propellant system. Past experience with the OF_2/MMH propellant combination indicates that the general water content level indicated for all of the propellant systems are nearly identical. At the indicated water concentration for these propellant systems, it is possible that it is of no special significance with respect to chamber chemical surface erosion. It has since been found that possible reactions can be anticipated with the boron-oxide species and carbon base chambers.

Radiative Cooling

The capability for nozzle radiation cooling is a direct function of the incident heat flux to the chamber wall. The prevailing heat flux will determine the area ratio at which a radiation skirt may be attached. Because the maximum radiative flux is a constant for a given nozzle geometry and a given wall material (fixed maximum wall temperature), a radiation attach factor can be developed to indicate the nozzle position

at which the heat flux has been reduced to a compatible level. This radiation attach factor can provide an index of suitability for radiation cooling. This factor is essentially coincident with nozzle heat transfer coefficient factors derived by the simplified Bartz analysis or other analytical assessment techniques.

For the propellants considered, all appear quite comparable with respect to radiation cooling.

RATING SUMMARY

In a comparison of the propellant combinations, the separate rating areas consisting of performance, operational aspects, and thrust chamber cooling are of prime importance. The comparison by individual areas show the strong and weak factors of each candidate propellant system. A separate comparison permits easy selection of the best propellant combination for a selected mission or requirement. It would be rare for a propellant combination to have the highest combined rating score for all of the categories considered. Instead, the specific propellant combination is more likely to be selected on the basis of its marked superiority over the candidate systems in a single evaluation area such as cooling or performance.

It has been shown that if performance alone were the selection criteria, OF_2/B_2H_6 would be selected because of its obvious superiority to the other propellants considered. For operational aspects, either OF_2/B_2H_6 or OF_2/CH_4 would be considered suitable candidates. The OF_2/MMH combination is reduced in ranking in this category primarily because of its temperature liquidus range. For thrust chamber cooling, MMH would be favored because of its lower combustion temperature, its relative superiority for regenerative cooling, and proven applicability to ablative thrust chambers.

PERFORMANCE INVESTIGATION

The three space-storable fuels selected for experimental evaluation were monomethylhydrazine (MMH), butene-1 (C_4H_8), and diborane (B_2H_6). Both MMH and C_4H_8 represent analytically determined optimum fuels within their respective hydrazine and light hydrocarbon chemical families for combination with oxygen difluoride (OF_2). Diborane was selected as a prime candidate fuel because of its proven exceptionally high performance.

The oxidizer of specific interest was OF_2. However, because of its high cost and hazardous characteristics, experiments were generally conducted with FLOX, a fluorine-oxygen mixture (70.4-percent fluorine and 29.6-percent oxygen). This particular FLOX mixture was demonstrated, both analytically and experimentally, to simulate satisfactorily the performance and heat transfer characteristics of OF_2. The major portion of the experimental work was therefore conducted with the 70-30 FLOX mixture, and OF_2 was used only when new concepts were tested.

As introduction to the performance studies, a summary of the basic performance characteristics for each of the three propellant combinations is helpful. The pertinent performance characteristics of OF_2/MMH, OF_2/C_4H_8 and OF_2/B_2H_6 are presented in Table 6 . The optimum mixture ratio, combustion temperature, molecular weight, and ratio of specific heats are tabulated for each propellant combination. The mixture ratio represents the optimum proportion for maximum performance and does not reflect consideration of propellant density effects on the deliverable payload. Density considerations would tend to shift optimum mixture ratios to slightly higher values.

The characteristic velocity for each propellant combination is dictated by the product gas temperature, molecular weight, and ratio of specific heats as shown in the equation below:

$$c^* = \frac{\sqrt{g_c \gamma RT}}{\gamma \sqrt{\left[\frac{2}{\gamma+1}\right]^{\gamma+1/\gamma-1}}}$$

TABLE 6

BASIC PROPELLANT PERFORMANCE PARAMETERS

Propellant Combination	Mixture Ratio	Temperature, F	Molecular Weight	Ratio of Specific Heats (γ)	Characteristic Velocity, ft/sec	Vacuum Specific Impulse* lbf-sec/lbm
OF_2/MMH	2.50	6640	19.2	1.31	6704	415.4
OF_2/C_4H_8	3.85	7240	20.0	1.33	6854	419.0
OF_2/B_2H_6	3.87	7130	18.2	1.29	7147	445.2

*At 100-psia chamber pressure with 60:1 expansion area ratio nozzle

From this expression, it can be seen that c* is proportional to $\sqrt{\frac{T}{M}}$ and to a function of the ratio of specific heats. For the expression shown, c* is a mild function of γ and increases slightly with decrease in γ. The values in Table 6 clearly show that the relatively high combustion temperature, low molecular weight and low γ favor OF_2/B_2H_6 for maximum c*. On the other hand the effect of temperature, molecular weight and γ for OF_2/MMH and OF_2/C_4H_8 offset one another and OF_2/C_4H_8 emerges as only slightly superior to OF_2/MMH. The relative performance levels are also reflected in the theoretical vacuum specific impulse for space operation with a 60:1 expansion area ratio thrust chamber operating at a chamber pressure of 100 psia.

Having established an absolute theoretical potential for each propellant combination, it is of further importance to consider the capabilities for attaining these maximum values. For most liquid bipropellant systems, c* efficiency is affected by both propellant vaporization and mixing. These two processes can be considered independently in their effects on efficiency. A close approximation of overall efficiency can be obtained from

$$\eta_{c^*} = \eta_{c^*,\ vap} \times \eta_{c^*,dist} \qquad (1)$$

where

η_{c^*} = the overall c* efficiency

$\eta_{c^*,\ vap}$ = the c* efficiency which would be obtained if propellant mixing were completely uniform, and the only losses were caused by incomplete propellant vaporization

$\eta_{c^*,\ dist}$ = the c* efficiency which would be obtained if propellant vaporization were complete, and the only losses were caused by nonuniform propellant mixing.

Analysis of the parameters which affect c* efficiency is therefore logically divided into considerations of $\eta_{c^*,\ vap}$ and $\eta_{c^*,\ dist}$.

PROPELLANT VAPORIZATION EFFICIENCY

The effects of incomplete propellant vaporization on c* efficiency can be quantitatively studied by means of an analytical propellant combustion model developed at Rocketdyne several years ago by Lambiris, Combs, and Levine (Ref. 1). This combustion model exists in the form of a Fortran IV Computer Program written for the IBM-360 computer. To determine the degree of propellant vaporization, the combustion model takes into consideration:

1. Compressible combustion gas flow with mass and energy addition
2. Droplet drag in the accelerating combustion gas flow
3. Droplet vaporization with convective heat transfer from the hot combustion gas

These factors result in an analytical description of the "bootstrap" combustion processes typical of rocket engines. The model calculates axial profiles of chamber pressure, combustion gas velocity, vaporization from a range of droplet sizes corresponding to the droplet size distributions produced by the injector, droplet velocities, and the overall percentage of fuel and oxidizer vaporized.

The combustion model calculates the compressible flow of combustion gases by the normal gas-dynamic equations, accounting for the effects of mass and energy addition from the vaporizing and reacting propellants.

Droplet drag, for the distribution of droplet sizes produced by the injector, is determined by the scalar equation shown below:

$$\frac{dV_D}{dt} = \frac{3}{4} \times \frac{C_D \rho_g (V_g - V_D)^2}{\rho_L D} \qquad (2)$$

where

V_D = droplet velocity, ft/sec

t = time, seconds

C_D = drag coefficient (a function of droplet Reynolds number)

ρ_g = combustion gas density, lb/ft^3

ρ_L = droplet liquid density, lb/ft^3

V_g = combustion gas velocity, ft/sec

D = droplet diameter, feet

Although the droplet acceleration due to drag is a bootstrap process and is highly dependent on the rate of droplet vaporization, a first approximation to the effect of aerodynamic drag may be determined by considering the physical properties of the product gases and the liquid droplets. The combustion gas density for each of the three propellant combinations can be based on the bulk conditions at their respective optimum mixture ratio and the nominal design chamber pressure of 100 psia. The liquid droplet densities would be evaluated at their respective saturation temperatures corresponding to the chamber pressure. For purposes of comparing propellant property effects the values for the drag coefficient, C_D, the velocity difference between gas and liquid droplet (V_g-V_d), and the droplet diameter, D, can be considered equal for all of the propellant combinations.

The values of the bulk gas density and those for the boiling fuel droplets are listed in Table 7 for OF_2/MMH, OF_2/C_4H_8, and OF_2/B_2H_6, respectively. It is apparent from the tabular data that the gas densities for all three propellant combinations differ only slightly; the OF_2/MMH combination has the highest gas density, and OF_2/B_2H_6 has the lowest. The liquid droplet density can be seen to differ by a factor of two, with MMH being twice that for B_2H_6, the lightest fuel. By noting the characteristics of the drag expression (Eq. 2) it is evident that the ratio of gas to liquid

density provides some index of the acceleration exerted on the liquid droplets. From their respective gas/liquid density ratios, it is evident that MMH would be least affected, while the much lighter B_2H_6 droplets would be almost twice as sensitive to acceleration due to aerodynamic drag. This comparison indicates that the "residence" or available time for fuel droplet vaporization in a combustion chamber is much more restricted for B_2H_6 than for the heavier MMH. To develop a comparable c* efficiency, the reduced available time in the combustion chamber must be compensated by a higher rate of propellant vaporization. A direct comparison can also be made of the relative drag effect on the liquid OF_2 droplets; however, because of its significantly higher densities (ρ = 1.52 gm/cc), it is much less sensitive than the fuels considered.

Droplet vaporization may be characterized by the following simplified expression:

$$\frac{d(D^2)}{dt} = k' = \frac{144 \times 8\lambda_g}{\rho_L C_{p_v}} \ln \left[1 + \frac{C_{p_v}}{\Delta H_v} (T_g - T_L) \right] \left(1 + 0.6 \, Pr^{1/3} \, Re^{1/2} \right) \quad (3)$$

Where

k' = droplet vaporization rate constant, in.^{2}/sec

D = droplet diameter

λ_g = combustion gas thermal conductivity

ρ_L = liquid density at the droplet boiling temperature

C_{p_v} = vaporized propellant heat capacity

H_v = liquid propellant heat of vaporization

T_g = combustion gas bulk temperature

T_L = liquid propellant boiling temperature

Pr = Prandtl Number for the combustion gas

Re = Reynolds Number for combustion gas

For computer solution of Eq. 3, the application is more complex. The simplified expression is presented here to show the effects of the various physical parameters on droplet vaporization rate. The last bracketed term on the right-hand side of Eq. 3 represents the effects of forced convective heating on droplet vaporization; the remainder of the terms represent the effects of propellant and combustion gas physical properties on droplet vaporization rate.

Because of the known monopropellant combustion characteristics of monomethylhydrazine, it cannot be classed as a true vaporization-rate-limited system depending solely on droplet heating, vaporization, and chemical reaction with the oxidizer. A vaporization-rate-limited combustion model thus tends to underestimate the true performance behavior of most hydrazine-type fuels. The monopropellants initially undergo an exothermic decomposition upon attainment of a relatively low critical temperature and subsequently react with the OF_2 oxidizer. The two-stage reaction is substantially more efficient than for those propellants which undergo a strict vaporization process. A reasonable comparison of the vaporization rates for C_4H_8 and B_2H_6 may be made, however, based on Eq. 3.

Both thermal conductivity and propellant vapor C_p are temperature and concentration dependent values which must be integrated from the liquid propellant boiling temperature to the combustion temperature. Although C_p is evaluated only for the propellant vapor itself, the thermal conductivity is evaluated for both the propellant vapor and reaction products. Low heat capacity and high thermal conductivity promote rapid propellant vaporization. The B_2H_6 system thermal conductivity appears to be slightly higher than that for C_4H_8 while C_p is essentially identical for either system. Thus, a comparison of C_p and λ_g for the two propellants indicate nearly equal k' values.

Other fuel properties such as the droplet saturation temperature at 100 psia chamber pressure, the sensible heat, and the latent heat of vaporization are listed in Table 8 . The sensible heat required to bring the

TABLE 7

COMPARISON OF BULK GAS AND FUEL DROPLET DENSITIES

Propellant Combination	Gas Density at 100 psia, gm/l	Fuel Density at 100 psia, gm/cc	(ρ_{gas}/ρ_{fuel})
OF_2/MMH	0.4039	0.740	0.546
OF_2/C_4H_8	0.3875	0.545	0.711
OF_2/B_2H_6	0.3579	0.365	0.981

TABLE 8

PROPELLANT PROPERTIES AFFECTING DROPLET VAPORIZATION

Fuel	Saturation Temperature at 100 psia, F	Heat of Vaporization Btu/lbm	Inlet Temperature, F	Sensible Heat, Btu/lbm
MMH	308	290	70	180
C_4H_8	135	135	70	40
B_2H_6	-56	185	-110	50

fuel from storage conditions to its boiling temperature is obviously smaller for diborane. The indicated total heat input requirement is also smaller for B_2H_6. However, considering the high bulk driving temperatures available, the effect on vaporization rate is negligible.

A major property difference is seen in the liquid fuel densities (Table 7). For equal fuel drop sizes, the much lower density of diborane indicates a higher surface area-to-mass ratio and thus faster vaporization. For equal fuel flowrate, this implies that a larger number of B_2H_6 droplets of a given size are produced.

In summary, it appears that B_2H_6 is superior to C_4H_8 in terms of vaporization rate. Drag considerations, however, indicate that the heavier C_4H_8 droplets have greater residence time in which to vaporize. The total effect of the various propellant properties is most effectively calculated by computer to determine the actual vaporization efficiency resulting from the complex interaction of gas dynamics, drag, and propellant heating.

By proper application of these input properties in the one-dimensional vaporization-rate-limited combustion model, the c* efficiency can be predicted for these specific propellant combinations. The curves of Fig. 7 illustrate the effect of propellant drop size (equal for both fuel and oxidizer) for OF_2/C_4H_8 and OF_2/B_2H_6 in a common thrust chamber configuration (L^* = 20 inches, A_c/A_t = 2.14). A prediction for OF_2/MMH is not included because of the monopropellant characteristics of MMH; the basic vaporization-rate-limited combustion model grossly underestimates its real performance potential. Sophistication and modification of the computer program to model the exothermic decomposition of MMH and subsequent reaction with the OF_2 oxidizer would provide a more realistic estimate of its basic performance characteristics.

The graphical display of OF_2/C_4H_8 and OF_2/B_2H_6 propellant combinations was based on their respective optimum mixture ratios at a common design condition of 100 psia chamber pressure. The vaporization efficiency is seen

to be a strong function of the initial propellant volume-mean drop size. The physical significance of this dropsize is not readily apparent. It is an empirically determined value assumed to exist at the injector end of the chamber and is used in the initial vaporization calculations.

Vaporization efficiency (a factor directly affecting the overall c* efficiency) is defined by the following expression:

$$\eta_{vap} = \left(\frac{\dot{w}_B}{\dot{w}_I}\right)\left(\frac{c^*_B}{c^*_I}\right)$$

The subscript B denotes the vaporized and reacted conditions in the chamber; the subscript I pertains to the initial injected condition. The first term in the product function is a measure of the amount of propellants actually vaporized, while the second ratio is a measure of the actual c* efficiency attainable at the mixture ratio of the vaporized propellants. The ratio $\dot{w}_B/\dot{w}_I$ is strongly dependent on the injected mixture ratio, dropsize, and propellant vaporization rates. Depending on the actual injection mixture ratio and the rate at which fuel and oxidizer is vaporized, the ratio $\left(\frac{c^*_B}{c^*_I}\right)$ could be smaller or larger than 1.0. The expression, η_{vap}, is an index of the actual propellant vaporization efficiency and constitutes a significant part of the simplified resultant c* efficiency.

It is readily apparent from the curves of Fig. 7 that the vaporization efficiency of FLOX/B_2H_6 is significantly higher than that for FLOX/C_4H_8, particularly with large initial drop sizes. This performance difference is a reflection of the various input parameters which define propellant drag, vaporization due to convective heat transfer, and the gas dynamics of the two-phase system. In addition to indication of vaporization efficiency, the curves in Fig. 7 also illustrate the effects of propellant drop size on vaporization sensitivity. Increases in chamber size will effect an increase in droplet residence time and resultant minimization of the vaporization loss. However, restrictions on chamber size may dictate engineering emphasis to decreasing the initial propellant drop size through improvements in propellant atomization.

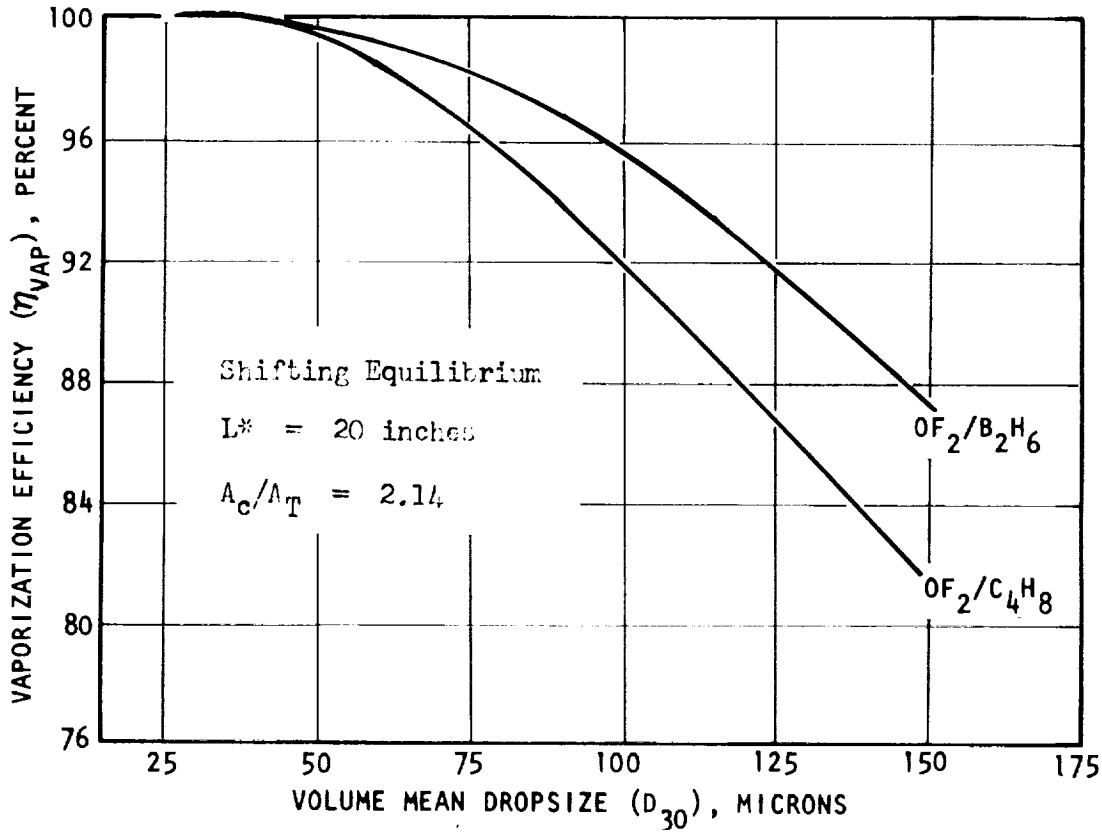

Figure 6. The Effect of Propellant Drop Size on Vaporization Efficiency for Two Candidate Spare Storable Propellant Systems

The process of propellant atomization can be considered as occurring in two complementary phases. Propellant atomization occurs initially through mechanical interaction of hydraulic streams and, subsequently, by shear forces exerted by the generated combustion products. For the injector type considered in this program, primary atomization occurs as a result of energy exchange through impingement of high velocity liquid propellant streams near the injector face. It is primarily controlled by injection velocity, impingement angle, orifice size, and pertinent liquid properties such as surface tension, viscosity, and density. Subsequent secondary atomization occurs as a result of the shearing forces developed by the velocity differences between the initially atomized liquids and the evolving reactant gases in the chamber. Significant parameters which affect gas velocity are the same as those which govern propellant vaporization rate. However, chamber geometry, chamber pressure, and mixture ratio are of prime importance. The resultant dropsize distribution is then heated and vaporized as it is accelerated through the chamber. The mean dropsize and the axial station at which vaporization begins (usually assumed to be 1 inch from the injector) are determined empirically.

For operation in injector/thrust chamber configurations of fixed design, it is often expedient to consider only the primary hydraulic atomization parameter by making the assumption that secondary atomization is not significantly perturbed. This analytical technique permits mechanical correlation of throttling performance through simple injection parameters such as $\sqrt{\frac{D}{V}}$. This simplication does not account for first-order changes in combustion gas density (affecting secondary atomization). Therefore, the resultant performance must be correlated by an index which includes the important secondary atomization parameters.

As an illustration of the effect of propellant atomization on performance, it is only necessary to consider the basic atomization expression developed by Ingebo (Ref. 2):

$$D_{30} = \frac{1}{K\sqrt{\frac{V_j}{D_j}} + K_2(|V_g - V_j|)} \qquad (4)$$

The primary (hydraulic) process is represented principally by the function $\sqrt{V_i/D_j}$ while the secondary (shear) process is affected by the droplet velocity lag ($|V_g - V_j|$).

For a fixed thrust chamber configuration and operating condition, propellant atomization can be influenced by a variation in the injector orifice size and jet velocity. In general, high velocity streams injected through small orifices improve atomization. However, the magnitude of the resulting adjustment in the secondary atomization term may offset the advantage.

Thrust chamber geometry variations can have strong influence on drop size through secondary atomization. Chamber contraction ratio has an approximately linear effect on combustion gas velocity. Thus, a decrease in ε_c by a factor of 2 doubles the gas velocity. Typical results in terms of vaporization efficiency are shown in Fig. 8 for OF_2/B_2H_6 at a chamber pressure of 100 psia and a mixture ratio of 3.65. Contraction ratio perturbations from 2.14 to 8.0 were made for chambers with lengths ranging between 3 and 10 inches. Because of the reduced residence time available, the performance was most sensitive to drop size in the shortest chamber. However, the importance of drop size can be emphasized by considering the predicted results in configuration A (ε_c = 2.14, L = 3.0 inches) and B (ε_c = 8.0, L = 10 inches). Configuration A has a predicted vaporization efficiency 1 percent higher than configuration B, despite having a characteristic chamber length (L*) of only 5.3 inches compared to 67.8 inches for B.

PROPELLANT MIXING EFFICIENCY

The effect of nonuniform mass and mixture ratio distribution is considered to be of importance equal to the vaporization process. Regardless of injector type, uniform mixing is a prerequisite for high combustion efficiency. In the absence of uniform mass and mixture ratio distribution, local fuel and oxidizer-rich regions will persist throughout the rocket chamber. Because of the short axial dimensions associated with rocket chambers, turbulent mixing and diffusion are relatively ineffective in

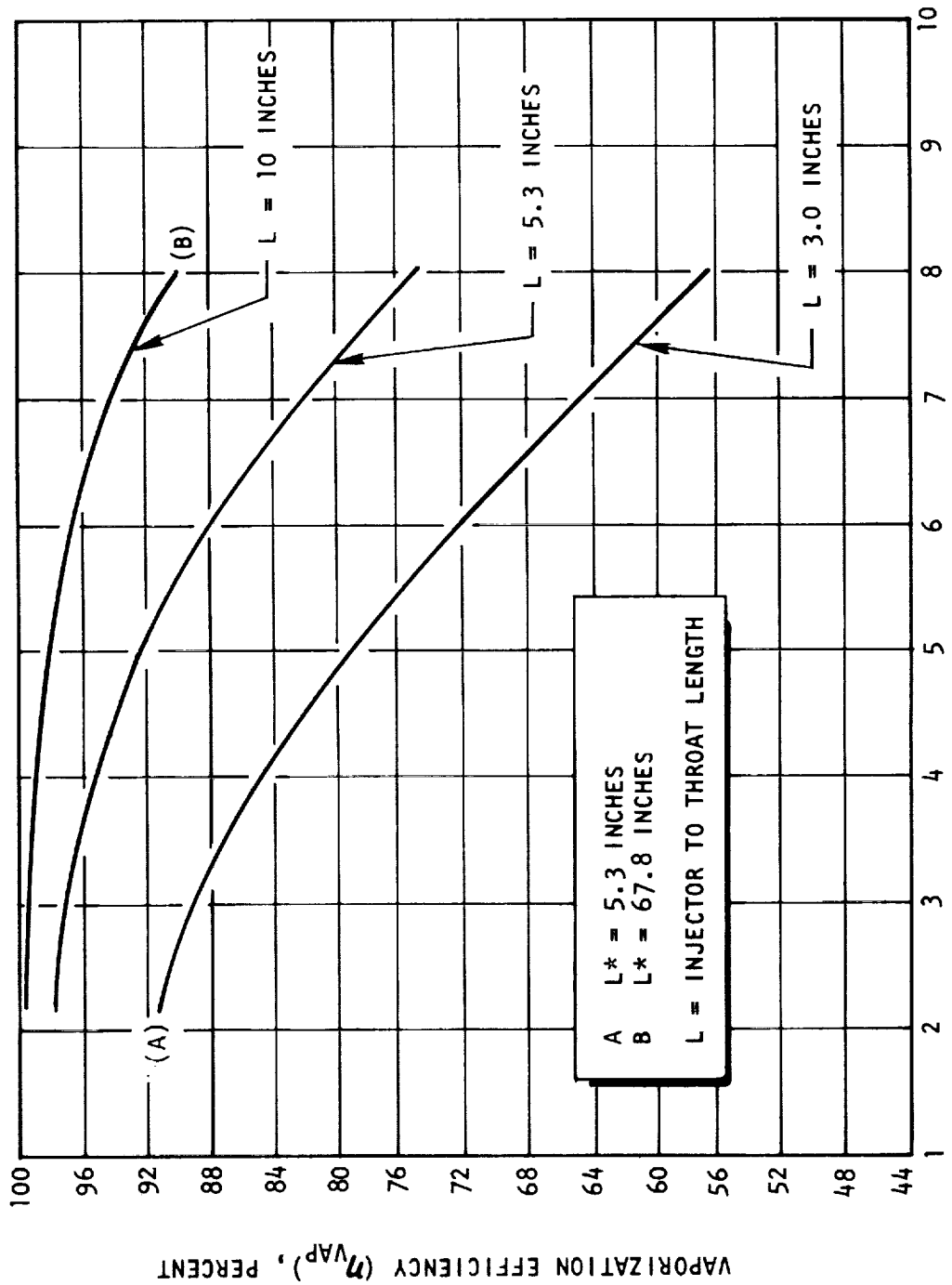

Figure 8. Contraction Ratio Effect on Vaporization Efficiency for OF_2/B_2H_6 at a Chamber Pressure of 100 psia, MR = 3.65

equilibration of propellant concentration. Consequently, the c* potential will be largely dependent on the initial distribution of fuel and oxidizer at the injector end of the chamber. Hence, if by cold-flow techniques the mass and mixture ratio can be determined for local regions within the chamber, the mixing efficiency can be predicted by applying simple mass weighted summation techniques.

For this program, the distribution analysis was based on a simplified stream tube model in combination with cold-flow experiments to determine distribution of propellants. The general features of the mixing model permit analytical consideration of an idealized rocket engine composed of N imaginary rocket chambers forming individual, isolated, stream tubes within the main chamber. Each stream tube is allowed to expand isentropically through the chamber and nozzle at its own mass and mixture ratio without heat or mass transfer to adjacent stream tubes. The c* efficiency due to mixing ($\eta_{c^*,dist}$) is determined by summation of individual mass weighted c* contributions of each individual stream tube and comparing the total to that theoretically attainable at the injected mixture ratio.

Correction factors for changes in specific heat ratio as a function of mixture ratio may be applied. However, if the effect of variation on the sonic point for each individual station can be neglected, the mixing c* efficiency can be expressed simply as

$$\eta_{c^*,dist} = \frac{\sum_{i}^{n} MF_i c^*_i}{c^*_{theo}} \qquad (5)$$

where

MF_i = the mass fraction in the individual stream being considered

c^*_i = theoretical c* corresponding to the mixture ratio of the local stream

c^*_{theo} = theoretical c* corresponding to the overall mixture ratio

The mixing quality can be expressed by an index, E_m, which defines the mass weighted deviation of local mixture ratio from initially injected overall mixture ratio. The index, E_m, was developed by Rupe (Ref. 3) and is shown below.

$$E_m = \left[1 - \sum_i^N MF_i \frac{(R - r_i)}{R} + \sum_i^N MF_i \frac{(R - \bar{r}_i)}{R - 1}\right] X\ 100. \qquad (6)$$

where

E_m = mixing index

MF_i = mass fraction in the stream tube

R = ratio of total oxidizer mass to total oxidizer and fuel mass

r_i = ratio of oxidizer mass to total oxidizer and fuel mass in an individual stream tube for $r_i < R$

$\bar{r}_i$ = ratio of oxidizer mass to total oxidizer and fuel mass in an individual stream tube for $r_i > R$

The foregoing expression for the distribution index is not universal because it is also functionally related to the injected mixture ratio. The c* efficiency due to propellant distribution, $\eta_{c^*,dist}$, is a function of both the distribution index, E_m, and the initially injected mixture ratio. The actual relationship between E_m, MR, and the resultant mixing c* efficiency is highly dependent on the theoretical performance characteristics of each propellant system.

The theoretical c* is shown in Fig. 9 as a function of mixture ratio for each of the propellant combinations. The theoretical curves are shown for the candidate fuels in combination with the FLOX (70-30) simulant rather than for the prime OF_2 oxidizer. A slight gain in absolute c* would be anticipated with OF_2; however, the characteristic trends are nearly identical. The optimum mixture ratio for maximum c* generally coincides with that for maximum specific impulse for most bipropellant

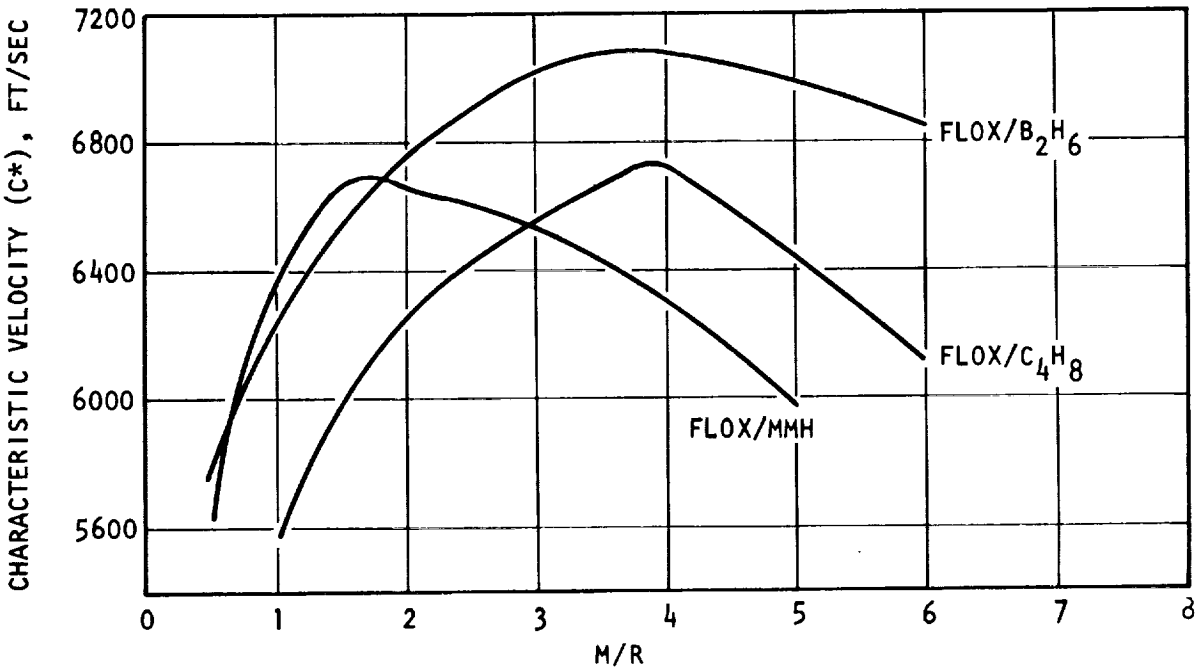

Figure 9. Characteristic Velocity Versus Mixture Ratio For Three Space Storable Propellant Combinations

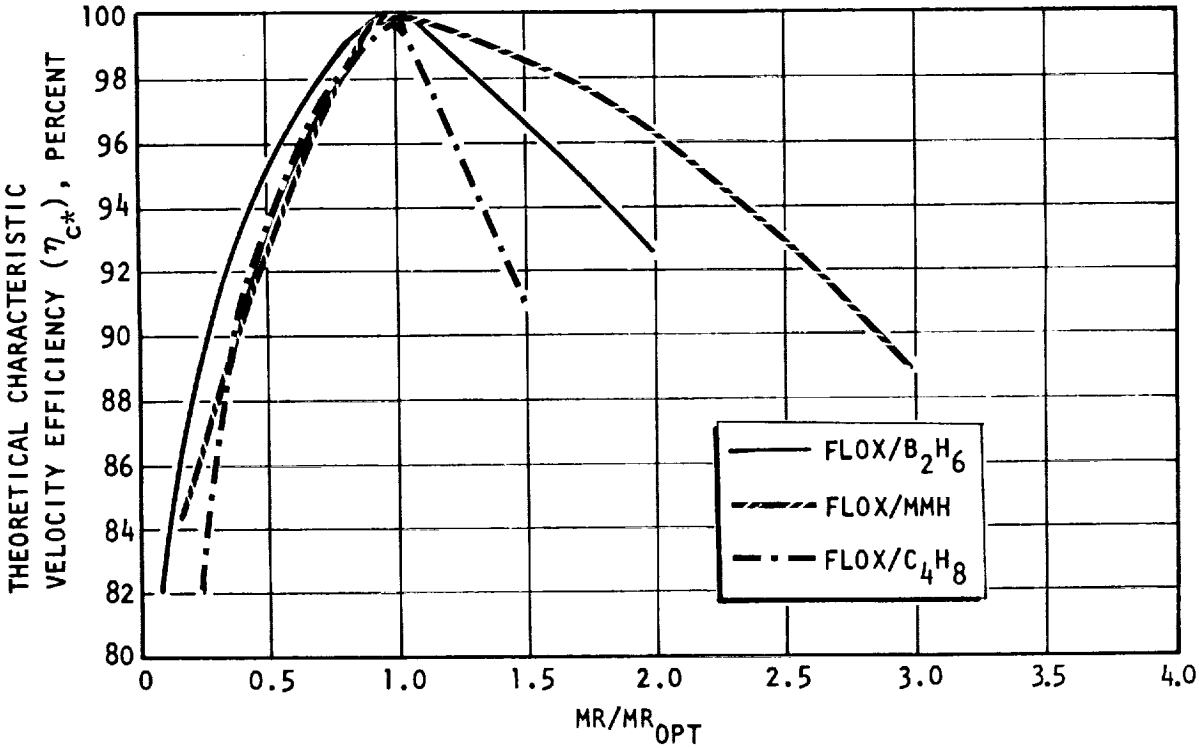

Figure 10. Theoretical c* Efficiency Corresponding to a Normalized Overall Mixture Ratio

combinations. It is important to point out that maximum I_s for OF_2/MMH optimizes at 2.5 rather than the indicated 1.8 mixture ratio for maximum c*. For OF_2/C_4H_8 and OF_2/B_2H_6, their respective optimum mixture ratio for c* and I_s are in close correspondence. Sensitivity to nonuniform distribution of propellants cannot be directly observed on examination of these theoretical curves. The task of comparing the relative sensitivity of each propellant is simplified by normalizing the mixture ratio ordinate to a ratio of actual to optimum mixture ratio and the abcissa to fractional values of their respective c* maximums.

In Fig. 10 , theoretical characteristic velocity index is replotted as a function of their respective mixture ratio functions, MR/MR_{opt}. It is readily apparent from these curves that OF_2/MMH is the least sensitive to off-optimum mixture ratio operation, while OF_2/C_4H_8 is shown by the steepness of the theoretical curve to be significantly more sensitive to perturbations in mixture ratio. It is of interest to point out that all of these candidate propellant systems have nearly the same characteristic at lower than optimum mixtures and that losses in c* are only amplified at higher than optimum mixture ratios.

Figure 10 is also useful for first order estimation of c* losses which would result from deliberate stratification of the injected mixture ratio distribution. In addition to a c* decrement resulting from local mixture ratio nonuniformities, a significant c* loss can occur because of combustion of a significant fraction of the total propellants at some reduced off-optimum mixture ratio. For stratification at a nonoptimum mixture ratio, local perturbations in mixture ratio tend to offset each other.

The effect of mixture ratio stratification on deliverable c* is indicated in Fig. 11 for the three candidate propellant systems. The curves illustrate the effect of deliberate striation of 30 percent of the propellants at various peripheral mixture ratio conditions, while the remaining 70 percent are injected at their respective optimum mixture ratios. It is evident from comparison of these curves, that OF_2/C_4H_8 would be most sensitive to deliberate mixture ratio striation.

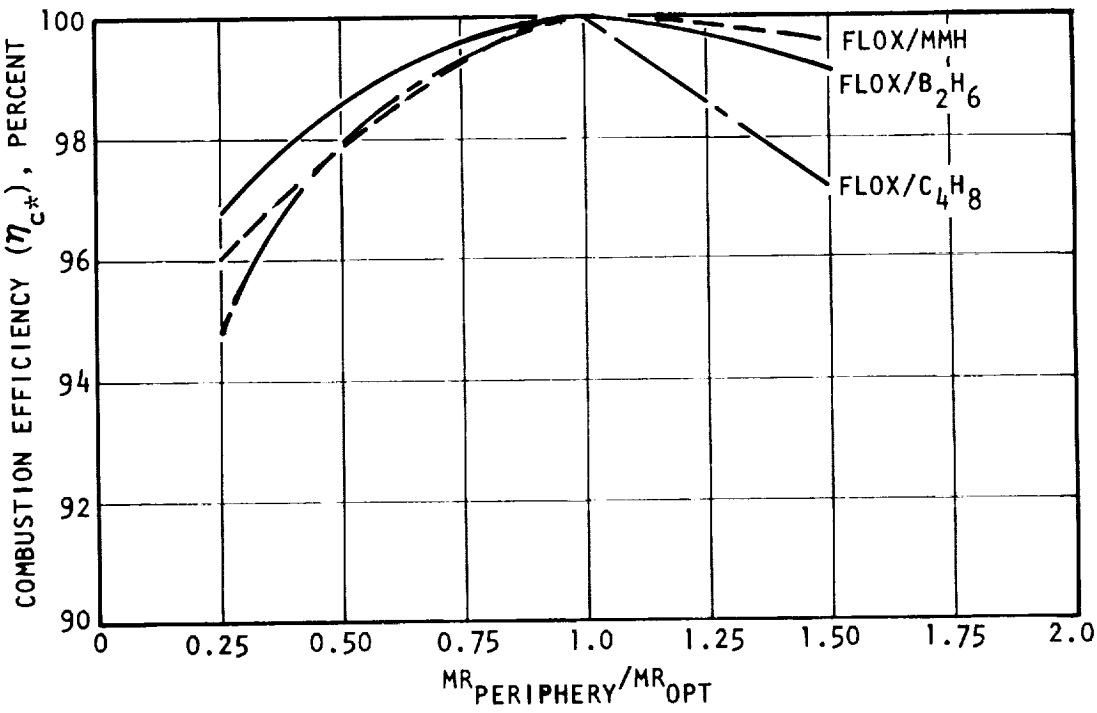

Figure 11. The Effect of Mixture Ratio Stratification on Performance for Three Candidate Space Storable Propellant Systems

It should be noted that deliberate low mixture ratio stratification of the peripherally injected propellants is common practice for attenuation of the thermal-chemical environment at the chamber wall. Reduction of the peripheral mixture ratio is generally accompanied by a corresponding reduction in local temperature and in the concentration of harmful oxidizing species. Deliberate reduction of the peripheral mixture ratio may be required for OF_2/C_4H_8 to reduce the tendency for deposition of free carbon on the thrust chamber wall. Similar procedures may be required for OF_2/B_2H_6 to reduce the tendency for condensation of corrosive oxidizing species on the thrust chamber wall.

This analysis indicates relative insensitivity of both OF_2/B_2H_6 and OF_2/MMH to a moderate level of nonuniform mixture ratio distribution. In addition, OF_2/B_2H_6 suffers only a moderate loss when severe mixture ratio stratification gradients are applied. These factors together with its inherently high c* make OF_2/B_2H_6 an attractive propellant combination for practical engine application where high performance is essential.

EXPERIMENTAL EVALUATION

During the course of the contract, extensive experimentation was performed to verify analytical design effort and provide empirical data for generation of injector and thrust chamber design criteria for OF_2/MMH, OF_2/C_4H_8, and OF_2/B_2H_6. Test data were obtained to characterize injector mixing performance, propellant vaporization efficiency, chamber heat flux profile, and long-duration injector/chamber compatibility under a variety of operating conditions and hardware configurations. The major portion of the tests was conducted under ambient conditions; however, a specific task was devoted to altitude performance evaluation of a thrust chamber (ε = 20:1) with monomethylhydrazine fuel. Extensive experimental data have been gathered for the three fuels, MMH, C_4H_8 and B_2H_6, with both the primary OF_2 oxidizer and FLOX (70-percent F_2) simulant.

Initial tests were conducted to determine the basic injector element design best suited for high performance in short chamber lengths with OF_2/MMH propellants. Three element types were chosen for evaluation: a self-impinging (like) doublet, an unsymmetrical two-on-two, and an unlike doublet. Full-size injectors employing these element types were fired at nominal mixture ratio (2.0) in copper calorimeter chambers of varying lengths. The results of these tests are presented in Fig. 12 . The unlike doublet injector provided significantly higher efficiencies in chambers of less than 6 inches in length. However, little difference could be observed in longer chambers at efficiency levels ($\geq$95 percent) considered adequate for use in either regenerative or ablative cooled engines.

The copper chambers used in the performance evaluation tests also provided a measure of the relative thrust chamber compatibility for the three injectors. Three independent rows of thermocouples were mounted on the nozzle; 15 on the long chamber section and 9 on the shorter section. A chamber schematic is presented in Fig. 13.

A plot of throat heat flux versus chamber length for the three injector types is shown in Fig. 14. Heat flux values were significantly lower in the thrust chamber as expected and generally followed the same trends indicated in Fig. 14. The lower heat flux profile produced by the like doublet injector is favorable for thrust chamber compatibility. Another point of injector comparison can be drawn from the relative circumferential uniformity of heat flux. The self-impinging doublet injector showed a rather uniform heat flux pattern while the unlike impinging patterns produced circumferential deviations of ±10 percent. The deviations result from local regions of varying mixture ratio near the wall and can adversely affect thrust chamber integrity by causing local peak loads.

No single injector produced vastly superior performance or compatibility characteristics. However, on the basis of its more uniform, slightly lower, chamber heat flux profile produced at no measurable c* degradation,

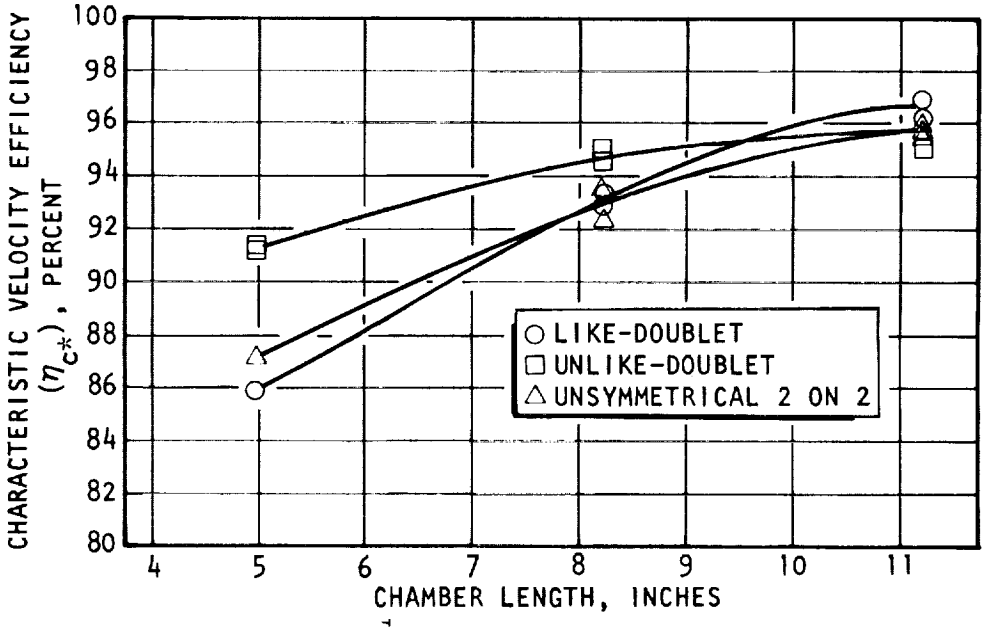

Figure 12. Results of Short Duration Tests Conducted With OF_2/MMH to Determine a Basic Injector Pattern

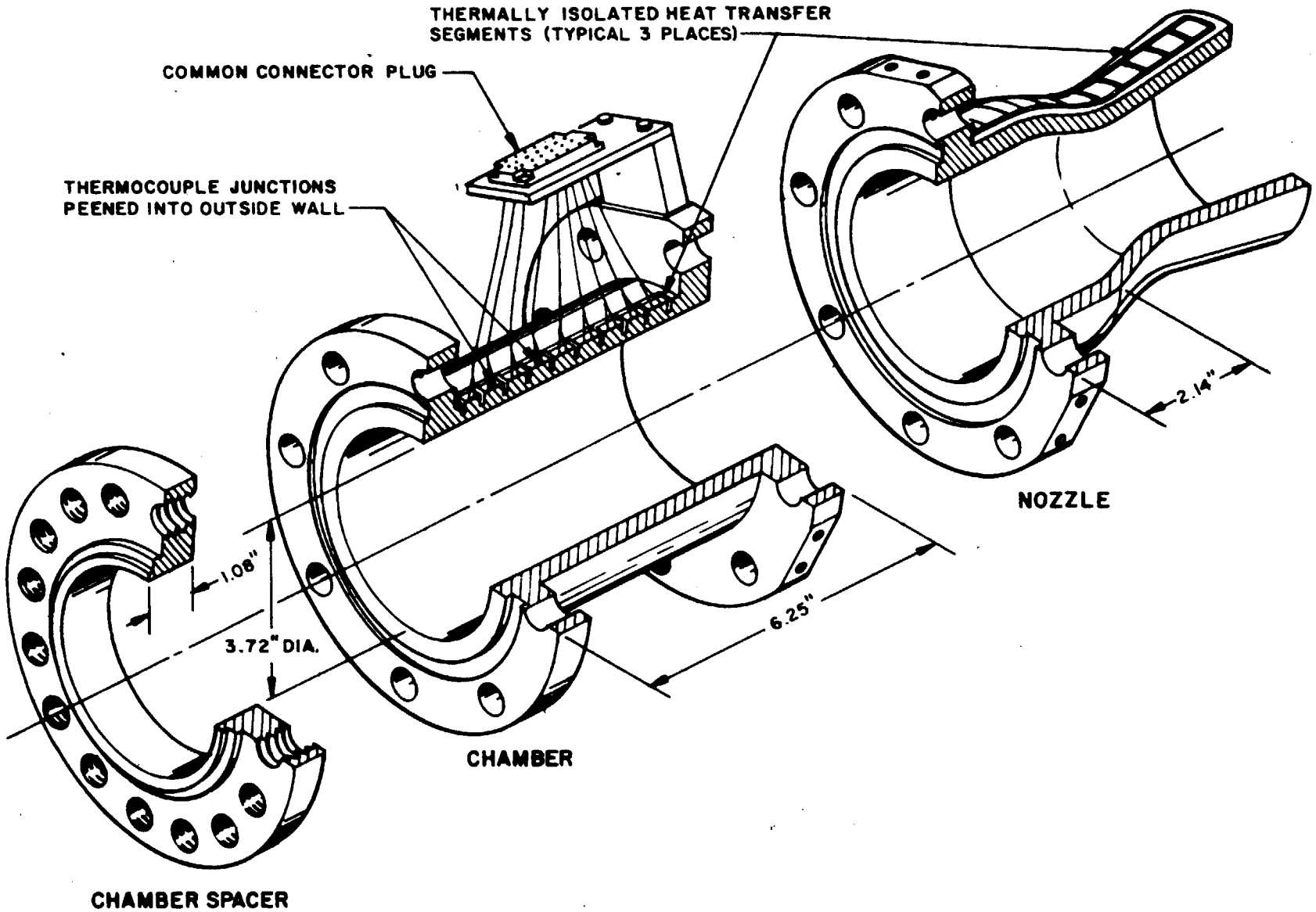

Figure 13. Uncooled Copper Calorimeter Thrust Chamber Used in Throttling Studies

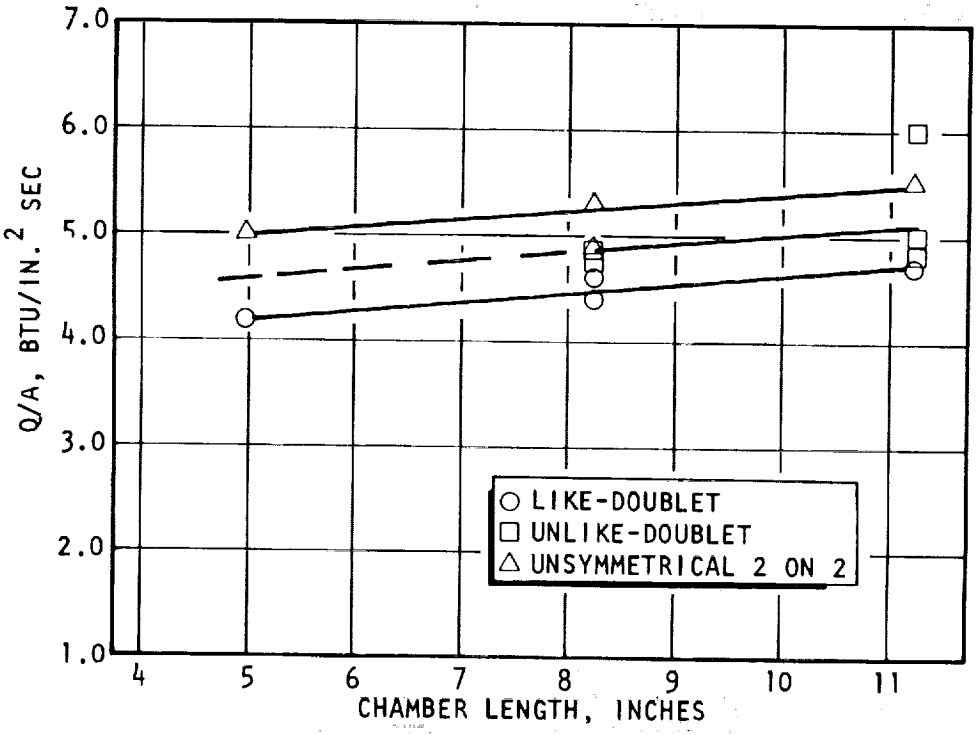

Figure 14. Throat Heat Flux Versus Chamber Length for Three Candidate Injector Types

the self-impinging doublet appeared to have a favorable combination of high-performance capability together with predictable thrust chamber compatibility.

An additional feature inherent in the like-doublet element design is the flexibility of pattern arrangement. To effect optimum mixing, high-performance combustion, a zero fan spacing arrangement (edge impinging fuel and oxidizer doublets) can be used. Conversely, mixture ratio gradation can easily be provided by increasing the fan spacing in a particular manner; for example, to provide a fuel-rich peripheral region at the wall. The alternating oxidizer-fuel ring pattern can be modified to provide the fan spacing and mixture ratio distribution required for a particular application.

The like-doublet injector pattern shown in Fig. 15 was used in the initial evaluation firings. Also, it was chosen as the basic design for all future injectors used during this program.

Performance evaluation tests with the three candidate space-storable propellant combinations were made with several injectors and thrust chamber contours at varying test conditions. The basic results can be quoted from tests made with the like doublet injector (Fig. 15 , with orifice sizes adjusted for mixture ratio) at a nominal chamber pressure of 100 psia. Figure 16 presents corrected c* efficiency data from tests conducted at nominal mixture ratio with each of the three fuels investigated. The results are plotted as a function of injector-to-throat length for a 2.14 contraction ratio copper chamber. Data points from tests utilizing both OF_2 and FLOX are included to show the characteristic similarity of these two oxidizers.

Since the injector and chamber hardware were identical in basic design, the variation in results shown in Fig. 16 reflect the efficiency of the combustion processes occurring with the several propellant combinations. The general similarity between the curves for B_2H_6 and MMH suggest that

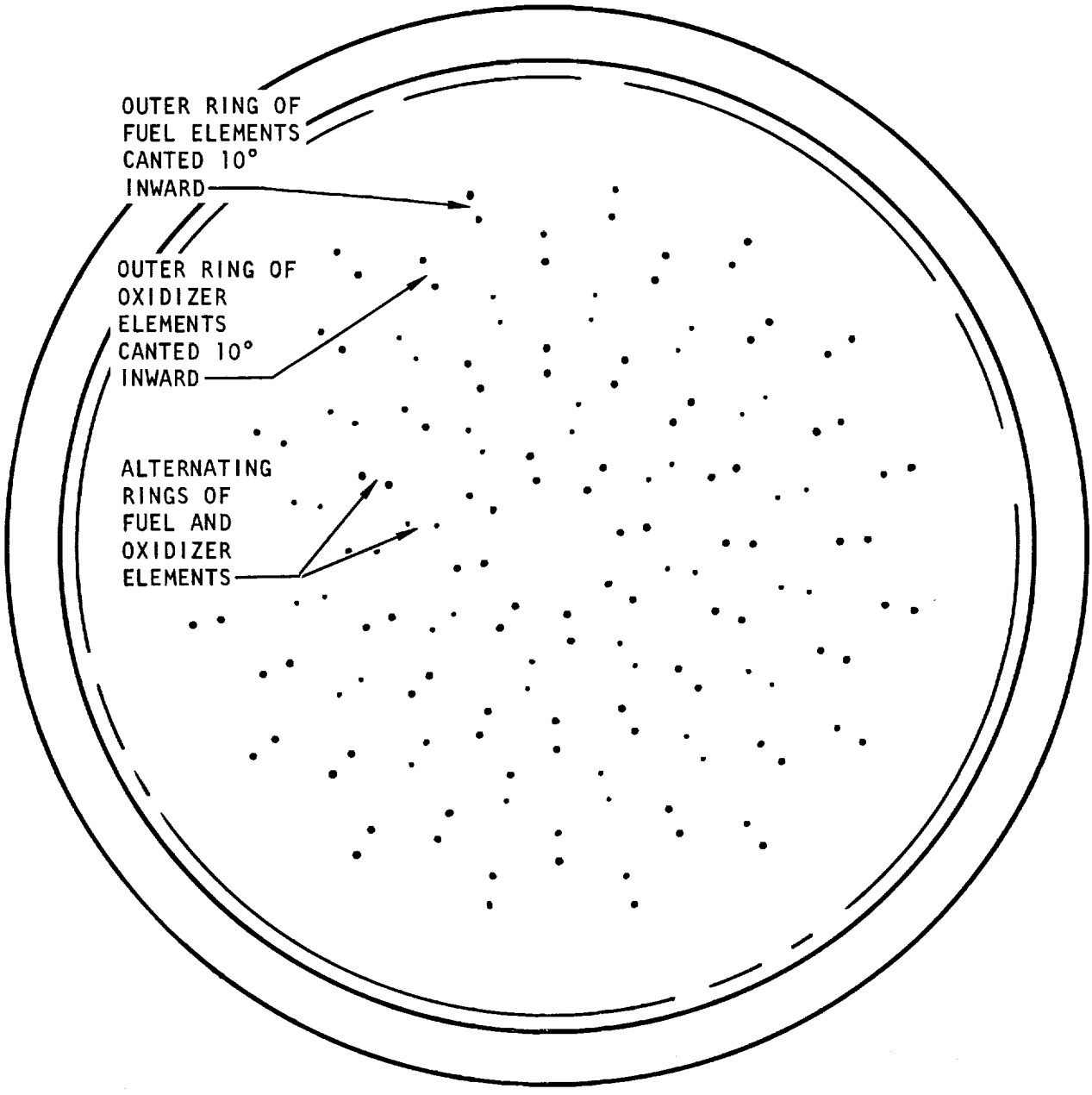

Figure 1. Orifice Pattern of Self-Impinging Doublet Injector (RID 2381)

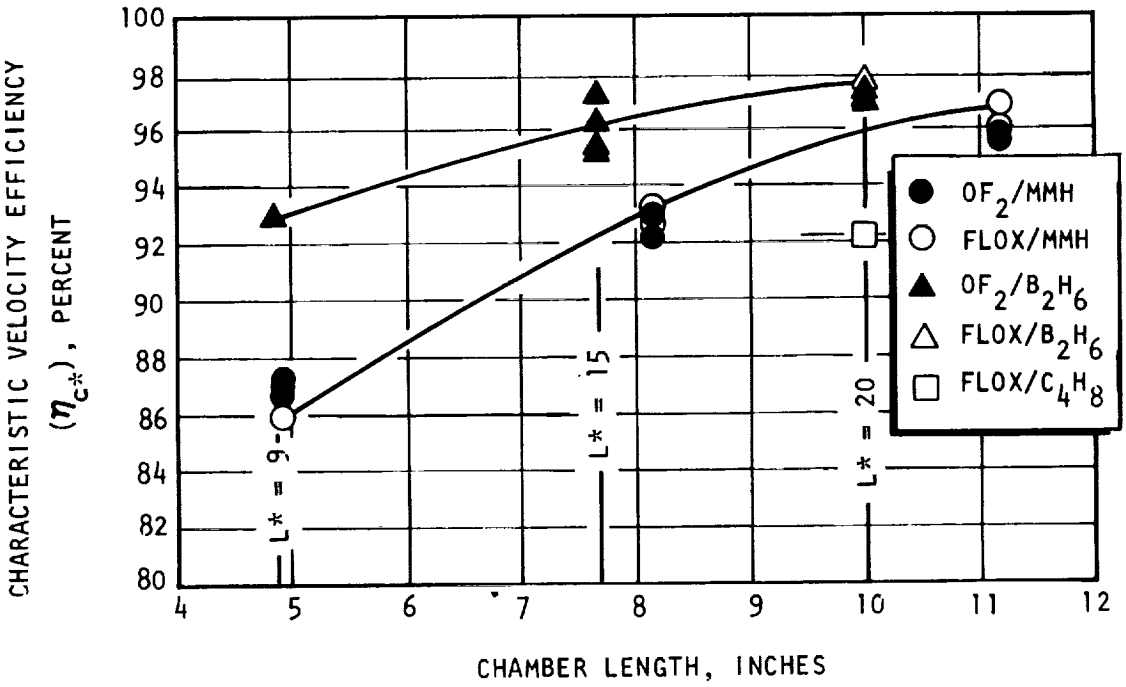

Figure 16. c* Efficiency Versus Chamber Length for Three Candidate Propellant Combinations, P_c = 100, Nominal Mixture Ratio

the performance shift is related to a vaporization lag. Both combinations are relatively insensitive to mixing losses (their approach to what appears to be a common asymptote indicates similar mixing efficiencies), but B_2H_6 vaporizes much faster than MMH. Butene-1 (C_4H_8) tests were run at only one chamber length; however, performance was significantly lower in the 20-inch L* chamber. Since the vaporization rate of butene-1 is higher than that for FLOX/MMH, the performance loss appears to have been caused by sensitivity to local nonuniformities in injected mixture ratio. Subsequent C_4H_8 tests made with an edge-impinging fan injector pattern (for improved mixing) produced over 97-percent efficiency in the same chamber.

Mixture Ratio Effect on Performance

Tests were also conducted to verify the c* performance dependence on mixture ratio as predicted in Fig. 9. In general, results followed the predicted trends, with the exception of tests made in short chambers ($\sim$ 5 inches). In this case performance is vaporization-rate limited and heavily dependent on drop size and propellant properties. Large mass flows of easily vaporized propellant, for example fuel-rich mixtures of FLOX/B_2H_6, more fully vaporize in the short chamber, resulting in peak delivered performance at lower than optimum mixture ratio. This phenomena had particular significance in determining test conditions for the OF_2/B_2H_6 interegen (internal regeneratively cooled) chamber demonstration. A low core mixture ratio ($\sim$ 3.0) was fired, producing peak performance at relatively low combustion temperatures and chamber wall heat flux.

Mass and Mixture Ratio Propellant Stratification. Several injectors employing various design distributions of fuel and oxidizer were fabricated and test fired. The objective was to improve injector/graphite chamber compatibility with OF_2/B_2H_6 by controlling the peripheral combustion temperature and concentration of corrosive chemical species. The orifices were sized and spaced to provide optimum mixing and performance potential in the core of the combustion chamber while maintaining a relatively cool, fuel-rich peripheral annulus of gases. The flexibility in design was made

possible by spacing the like-doublet elements as shown in Fig. 17 . As shown, the two central rings (injector core) are composed of edge impinging oxidizer and fuel fans designed to flow at the optimum (3.85) mixture ratio. The outer ring of oxidizer and fuel doublet (periphery) are spaced such that a fuel-rich annulus is adjacent to the wall and, further, the periphery is flowed at a reduced mixture ratio (typically 0.5 to 1.0 for OF_2/B_2H_6). A limited variation in peripheral mass percentage was also evaluated.

The stratified injector design approach was used in most of the long-duration B_2H_6 firings employing carbon base chamber materials. In addition, a high chamber pressure (500 psia) long-duration FLOX/MMH graphite chamber was cooled in this manner. Typical stratified injector performance results for FLOX/B_2H_6 are shown in Fig. 18. Here, c* efficiency, referenced to optimum theoretical at 100 psia chamber pressure, is plotted as a function of peripheral mixture ratio for varying core periphery mass distributions. All tests were conducted at the optimum core mixture ratio (3.85) in 20-inch L* chambers.

The test data plotted in Fig. 18 were obtained with an identical injector pattern (Fig. 17), with orifice size changes made to create the design propellant distribution. Thus, except for minor atomization effects, the results should reflect only the influence of propellant maldistribution on performance. At a peripheral mixture ratio of 3.85, the injector is unstratified and a maximum deliverable c* efficiency of 97.8 percent is obtained. For the 70-percent core, 30-percent periphery mass distribution, respective peripheral mixture ratios of 1.0 and 0.5 produce about 95-percent and 92.5-percent c* efficiencies. The 80-20 mass distribution yields slightly higher results as indicated. It is significant that even with 30 percent of the propellants injected at a 1.0 mixture ratio, FLOX/B_2H_6 is sufficiently insensitive to mixture ratio effects to deliver over 95 percent of theoretical optimum characteristic velocity. Further reduction in peripheral MR causes more drastic performance losses but the principle of stratification appears feasible from a performance standpoint. The extent of stratification required, of course, depends on wall material properties, particularly the resistance to chemical reaction in the resultant chemical and thermal environment.

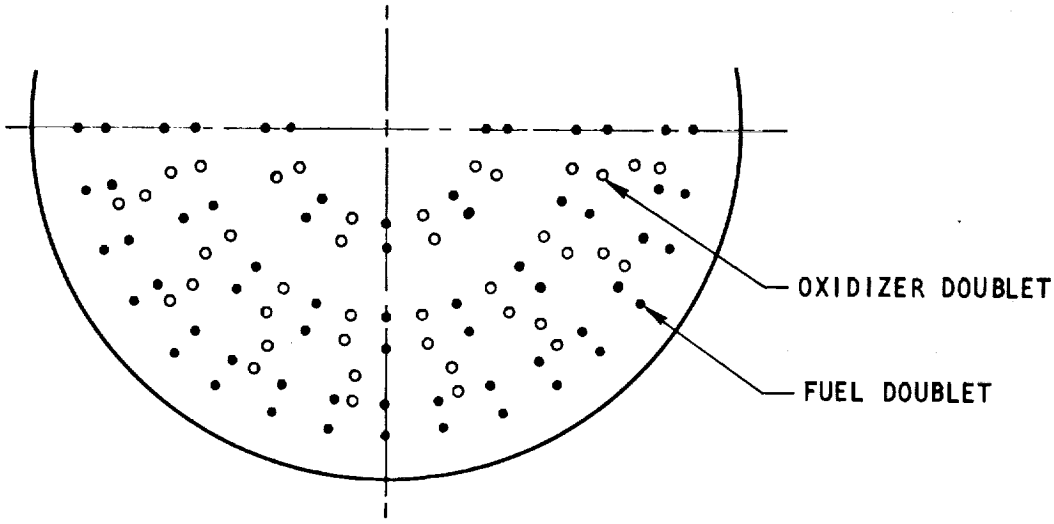

Figure 17. Typical Stratified Injector Face Pattern Incorporating Aligned Fuel and Oxidizer Fans in Core Region, Alternating Fans in Periphery

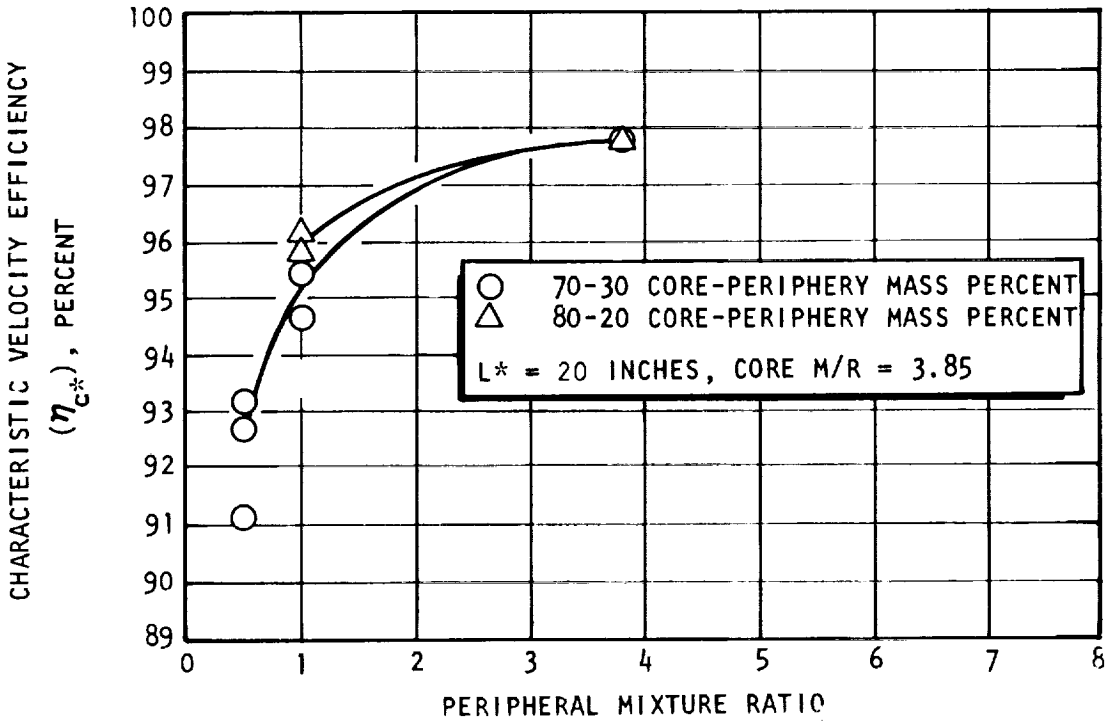

Figure 18. Effect of Peripheral Mass and Mixture Ratio Stratification on c* Efficiency

Throttling

One of the most important duty cycles required in a typical space mission performance envelope involves the capability for continuous throttling. Typically, the rocket engine system must be capable of throttling over at least a 10:1 thrust range while maintaining maximum performance efficiency.

Considerable effort was expended during the program to develop an efficient, continuously throttleable engine using OF_2/MMH. In addition, fixed point throttle data were obtained with both FLOX/butene-1 and FLOX/B_2H_6. The approach used was to effect 10:1 throttling capability using the dual-manifold combined area-pressure step throttling technique. In this method, the secondary fuel and oxidizer manifolds are first throttled alone, followed by flow reduction in the primary manifolds. Thus, from a condition of full flow in all available orifices at maximum thrust, the secondary fuel and oxidizer orifices are throttled simultaneously. At a selected chamber pressure these flows are cut off completely and throttling of the primary elements is begun.

Figure 19 is a schematic of the manifold design and orifice pattern chosen for OF_2/MMH. The selection of primary and secondary orifice spacing was dictated by the requirement that mixing efficiency be invariant with chamber pressure and that sufficient cooling be available to the injector throughout the throttle cycle.

Tests were conducted in 20 inch L*, 2.14:1 contraction ratio chambers with each of the three propellant combinations. The data were correlated with the primary atomization parameter, $\sqrt{D_i/V_j}$, since under these test conditions secondary atomization effects are nearly invariant. Only FLOX/MMH was continuously throttled. Furthermore, a different injector was used in FLOX/B_2H_6 tests; thus the data are not directly comparable. However, if a common injector is chosen and all data are normalized to correlate with the measured mixing efficiency, the resulting performance profiles can be calculated for each propellant combination.

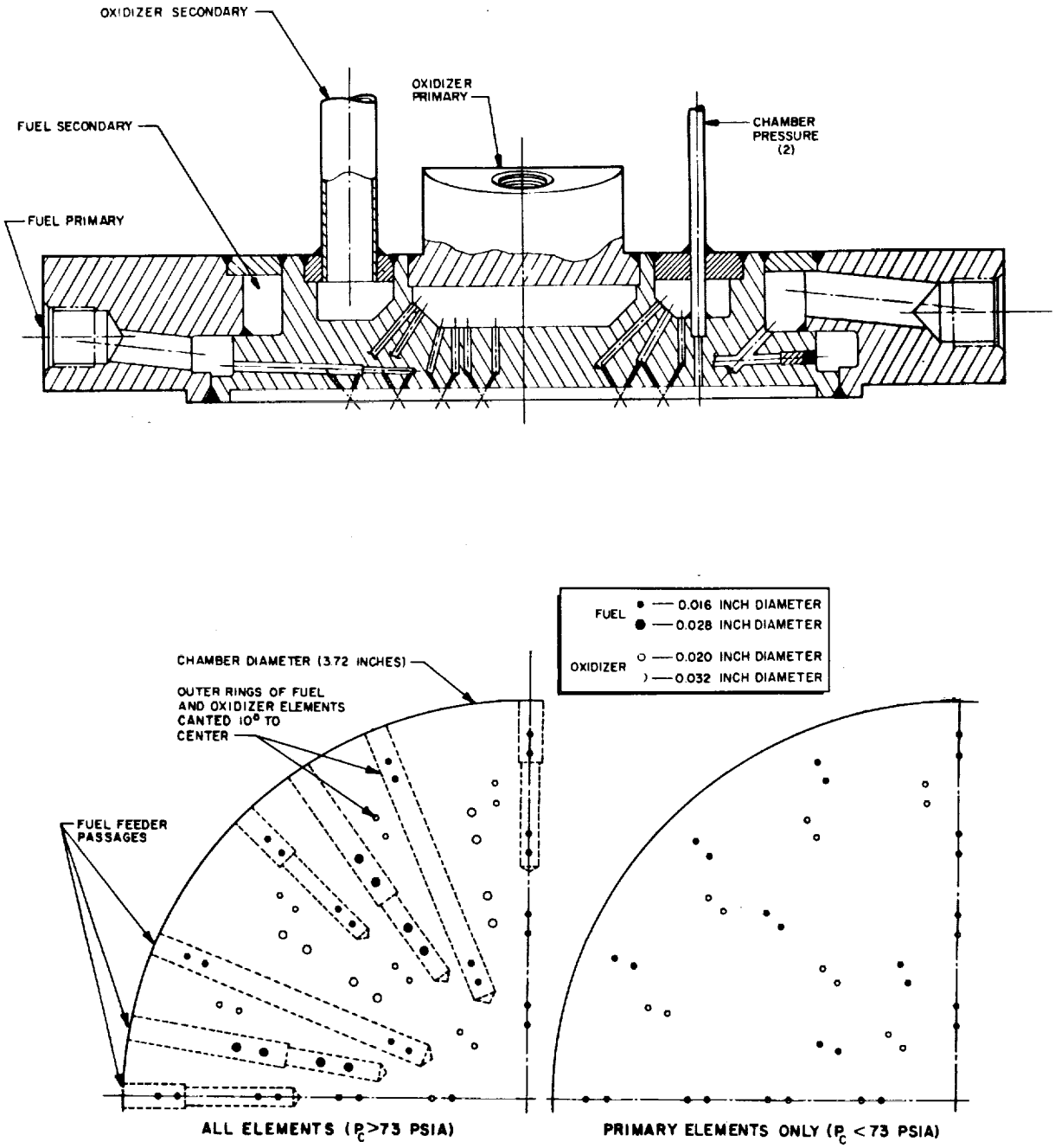

Figure 19. Dual-Manifolding Scheme and Orifice Pattern of the 96 Element, Self-Impinging-Doublet Throttling Injector

The injector chosen to normalize the data was a like-doublet, aligned fan pattern similar to that shown in Fig. 17 . Cold-flow results indicate that mixing efficiencies of 99 percent for FLOX/B_2H_6 and FLOX/MMH and 98 percent for FLOX/C_4H_8 can be expected with such a design. Therefore, normalizing all data such that η_{c^*} asymptotically approaches the corresponding mixing efficiency at low values of $\sqrt{D/V}$ (very fine atomization), and assuming all orifice sizes to be 0.020 inch in diameter with a maximum manifold pressure of 300 psia, the curves in Fig. 20 can be plotted.

The performance variation presented in Fig. 20 is assumed to be controlled entirely by vaporization efficiency. The upper two curves have a maximum deliverable efficiency of 99 percent (due to mixing losses); the lower curve has a maximum of 98 percent. The peculiar shape of the curves is a result of the atomization process associated with the throttling cycle. At 150 psia, all the orifices are flowing at pressure drops of 150 psid. As secondary propellant throttling is initiated and chamber pressure is lowered, the primary orifice pressure drop increases, aiding atomization, while secondary pressure drop decreases, retarding atomization. The mass weighted c* efficiency is gradually reduced until just before secondary flow cutoff, at which point nearly all propellant flow is primary. Peak performance occurs at secondary flow cutoff because the remaining propellant is injected at the maximum pressure drop (225 psid). From this point the throttling process is repeated with the primary flow only. At low chamber pressure the vaporization losses can be significant.

The relative positions of the curves in Fig. 20 are determined partially by mixing loss and partially by sensitivity to drop size. FLOX/MMH appears to be the least sensitive to drop size variations (relative flatness of profile), probably because of the monopropellant characteristics of MMH. FLOX/B_2H_6 appears to be slightly less sensitive to atomization effects than FLOX/C_4H_8, partially because of the greater vaporization rate of the fuel and also because of the higher injection velocities of the fuel (low B_2H_6 density). In any case the general characteristics of

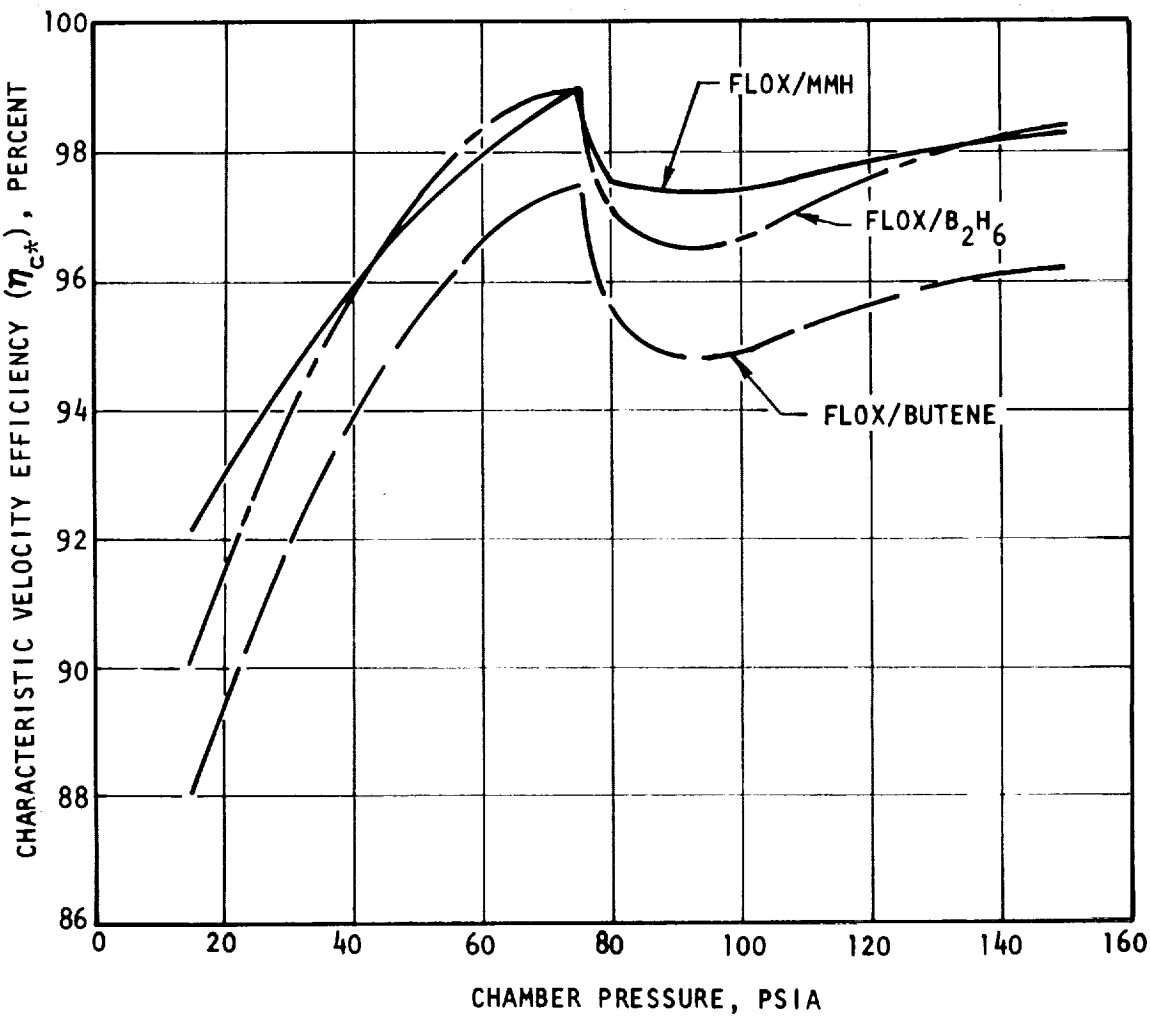

Figure 20. Throttle Cycle Performance Profile for Three Space Storable Propellant Combinations

the curves are similar and c* efficiencies greater than 95 percent are attainable over most of the throttle range. Optimization of the orifice sizes and chamber length should enable improvement of the low pressure performance values.

Altitude Performance Firings

A series of tests were made under simulated altitude test conditions firing both OF_2 and FLOX/MMH in a 20:1 expansion ratio chamber. Tests were conducted over a chamber pressure range of 63 to 150 psia. Diffuser limitations restricted the chamber pressure range over which available thrust data could be obtained. The injector employed for these tests was the standard like-doublet pattern shown in Fig. 15. All tests were conducted at a nominal 2.0 mixture ratio.

The performance results are plotted in Fig. 21 . The upper graph indicates the c* or combustion efficiency as a function of chamber pressure. Since the characteristic velocity is unaffected by nozzle flow conditions, performance results were obtained over the entire range of chamber pressures tested. The loss in η_{c^*} with reduced chamber pressure can be largely attributed to a reduction in the degree of primary atomization, as determined from fixed-point throttling tests.

The second curve in Fig. 21 presents the vacuum thrust coefficient efficiency versus chamber pressure. No change in nozzle expansion efficiency could be detected over the chamber pressure range tested.

Finally, the third curve shows the variation of specific impulse efficiency with chamber pressure. The indicated trend of slightly lower I_s with reduced chamber pressures reflects the above mentioned trend of characteristic velocity. The level of delivered I_s is below 90 percent. However, these performance values are uncorrected for chamber heat loss. At the higher wall temperatures experienced in long-duration firings the reduced heat loss will raise the specific impulse above 90 percent. In addition,

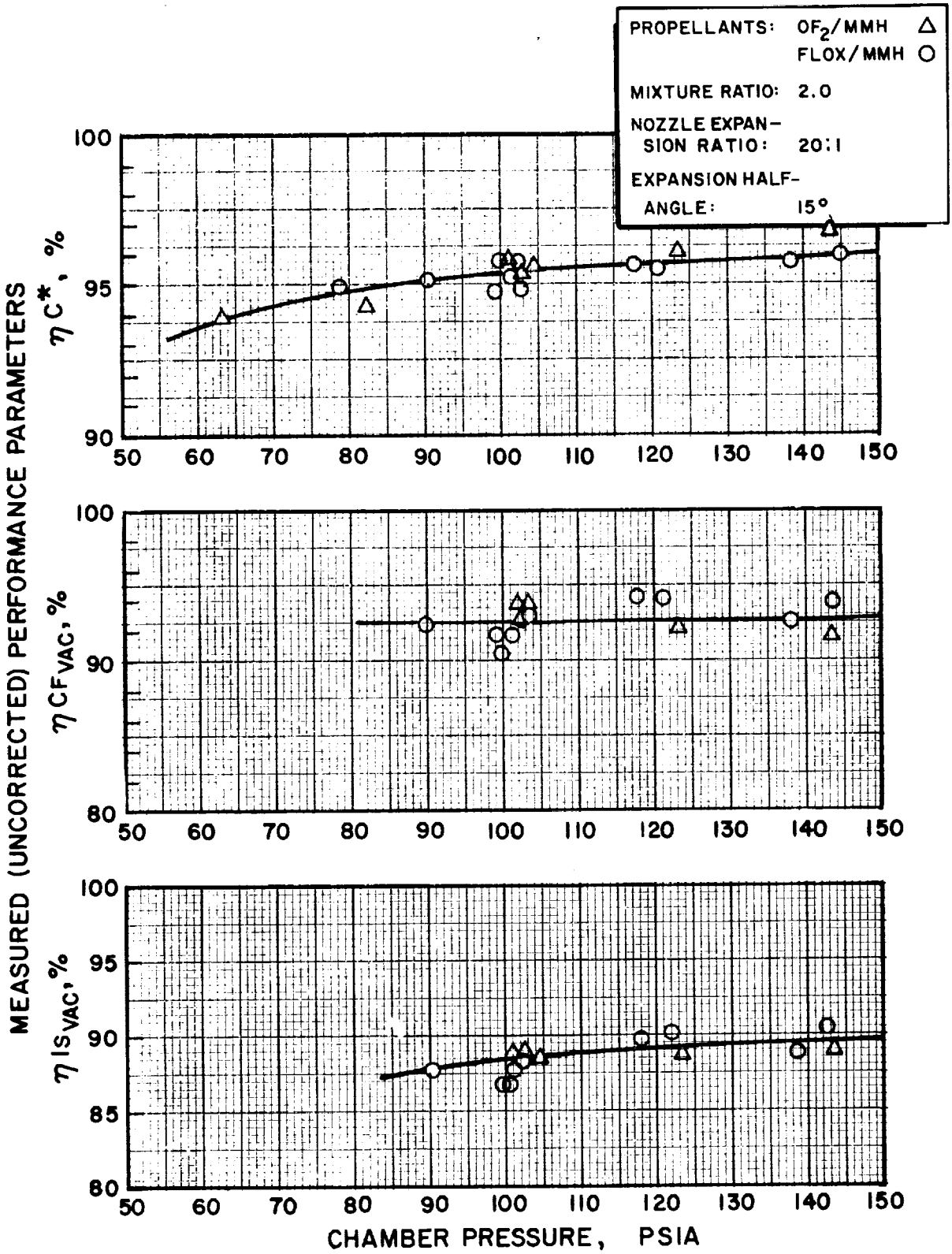

Figure 21. Measured Performance Parameters Obtained Under Simulated Altitude Conditions With the OF_2/MMH and FLOX/MMH Propellant Combinations

it is expected that an optimum contour (bell) nozzle would reduce losses another 2 percent. These conclusions apply directly to the OF_2/MMH propellant combination. The test data in Fig. 16 show the general performance consistency obtained with the OF_2 and FLOX oxidizers.

Performance Prediction Analysis

Continuous attempts have been made during the course of this program to correlate test results with all three propellant combinations. Several tools have been applied in these correlations, including cold-flow distribution tests, chamber geometry variations, and atomization studies. The final product has been the development of a c* performance analysis applicable to the general class of liquid propellants.

The basic supposition in the analysis is that c* losses are the result of separately measurable mixing and vaporization losses. Cold-flow distribution measurements are used to determine the injector mixing efficiency. A vaporization rate-limited combustion model is used to predict losses due to incomplete propellant vaporization. The latter class of performance losses has been related to injector hydraulics, propellant properties, and chamber conditions (operational and geometrical). Thus a method has been devised to determine (1) the mass and mixture ratio distribution at which combustion occurs, (2) the degree of atomization, and (3) the rate of propellant vaporization for a given injector/chamber condition and propellant combination. Thus, it becomes feasible to optimize the entire rocket engine configuration, including both design and operational conditions, subject only to mission and vehicle requirements.

HEAT TRANSFER INVESTIGATION

A first approximation of the heat transfer characteristics for the candidate space-storable propellant combinations may be made by estimating the effective gas-side heat transfer coefficient for the reaction products. By isolation of pertinent transport properties for each system, a rough approximation may be obtained to compare relative characteristics of each propellant system. Using the simplified Bartz analysis for fully developed turbulent flow, the effects of the gas properties on the heat transfer coefficient can be determined. As shown in Table 9, the values of gas viscosity, μ, specific heat, c_p, and Prandtl number, Pr, are of importance. The Reynolds number determinant is c* and the boundary layer property correction factor, σ, is a function of the ratio of specific heats, γ, and T_o, the gas total temperature. As can be seen from Table 9 the lower gas specific heat for OF_2/C_4H_8 in comparison to that for OF_2/MMH results in a lower value for the heat transfer coefficient (h_g) while just the opposite is true for OF_2/B_2H_6. The boundary layer correction is essentially the same for all three propellant combinations.

A first approximation to an estimate of heat flux indicates that OF_2/C_4H_8 would have a Q/A value approximately 3 percent higher than that for OF_2/MMH while OF_2/B_2H_6 would be close to 17 percent greater. These anticipated higher heat flux potentials result primarily from the higher differential between the adiabatic wall temperature and a common thrust chamber wall temperature of 1500 R. Thus, the lower value of h_g for OF_2/C_4H_8 is offset by the substantially higher ΔT while the high ΔT for OF_2/B_2H_6 tends to magnify the anticipated heat flux, due to the high h_g.

The heat transfer characteristics for each of the propellant combinations were determined for the thrust chamber throat and are based on frozen equilibrium properties at the throat. The effects of recombination and deposition of condensible species were neglected and are recognized to be potentially critical factors governing the actual heat flux rates. The results of experiments show that actual heat flux tended to follow the relative order of the anticipated heat flux level, but were otherwise substantially higher than analytically predicted.

TABLE 9

PARAMETRIC HEAT TRANSFER ANALYSIS (P_c = 100 psia)

$$\text{Heat Flux } (Q/A) = \left(\frac{\mu^{0.2} \quad C_p}{P_r^{0.6} \quad c^{*0.8}}\right) \sigma \; X(T_{aw} - T_w)^*$$

Propellant Combination	Mixture Ratio, o/f	Ratio of Specific Heat (γ)	Adiabatic Wall Temperature, R	Relative Heat Flux, $(Q/A)/(Q/A)_{OF_2/MMH}$
OF_2/C_4H_8	3.85	1.32	7707	1.033
OF_2/MMH	2.50	1.31	7106	1.000
OF_2/B_2H_6	3.87	1.28	7585	1.169

*$(T_{aw} - T_w) = (T_c - 1500)$

T_c = Combustion gas temperature

The actual measured heat flux for the three propellant combinations is shown in Fig. 22. The data shown are for FLOX/MMH, FLOX/C_4H_8 and OF_2/B_2H_6 for tests conducted in a common thrust chamber and with a conventionally designed 80-element, self-impinging injector having an identical pattern arrangement. FLOX (70-percent fluorine, 30-percent oxygen) has been shown to simulate the heat flux characteristics of OF_2 in combination with MMH and B_2H_6. As can be seen from Fig. 22, the MMH system has a peak heat flux of approximately 3.7 Btu/in.^{2}-sec at the throat while that for FLOX/C_4H_8 is about 5.7 and for OF_2/B_2H_6 about 7.4, or 54 and 100 percent of that for FLOX/MMH, respectively. Simple convective heat transfer analysis indicate respective increases of only 3 and 17 percent. Observed deposition of carbon with FLOX/C_4H_8, and B_2O_3 with OF_2/B_2H_6 would tend to indicate additional heat load due to species condensation on the chamber wall. Another factor which would result in a higher heat load would be recombination of species and resultant heat liberation.

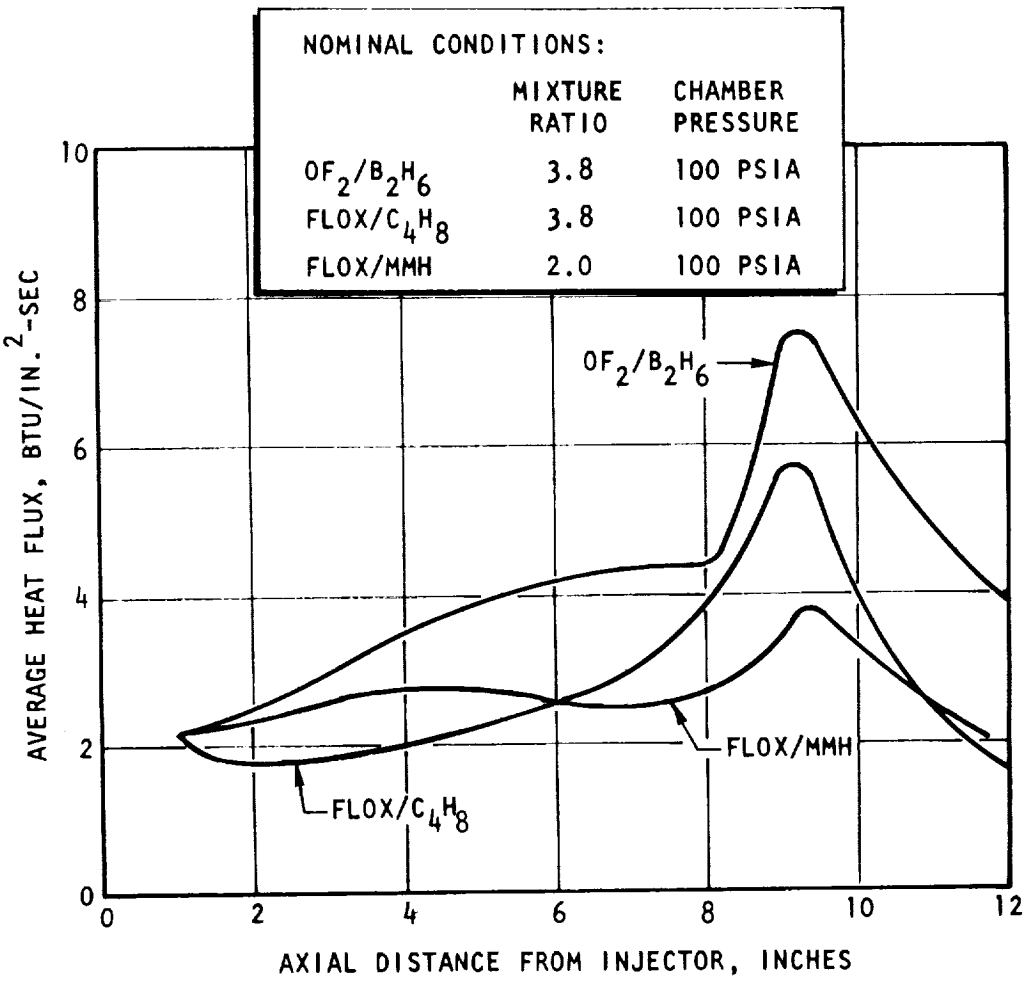

Figure 22. Comparison of Chamber Heat Flux Distribution From Firings With Conventional-Pattern, 80-Element Injectors Using OF_2/B_2H_6, $FLOX/C_4H_8$ and FLOX/MMH Propellants

SIMULATION OF OF_2 WITH FLOX (70 PERCENT F_2)

In the interest of reducing experimental costs, a major portion of all testing was conducted with FLOX (70/30) as a simulant for the much more expensive OF_2 oxidizer. To justify its use as a substitute for OF_2, both performance and heat transfer experiments were conducted to verify its suitability for OF_2 substitution. Early heat transfer studies of OF_2 with FLOX (70-30) in combination with MMH have demonstrated that both oxidizer behave almost identically as far as heat transfer characteristics are concerned. The near identical heat transfer characteristics with the two oxidizers is shown in Fig. 23. Similar characteristics were also determined for both FLOX and OF_2 in combination with diborane, B_2H_6. For C_4H_8, only FLOX was used during the experimental study because of nonhypergolicity of the OF_2/C_4H_8 combinations and requirements for an auxiliary ignition system.

SELECTION OF BASIC INJECTOR

During the early phases of the experimental program several injector candidates were considered for use with the OF_2 oxidizer and MMH fuel. The basic objectives of the program were to determine design criteria for a thrust chamber assembly capable of operating for 1800 seconds duration with a minimum performance of 95 percent of theoretical c*. Based on previous work, an unlike impinging doublet, an unsymmetrical two-on-two (two adjacent fuel streams impinging with two adjacent oxidizer streams at a common central point), and a self-impinging doublet design were selected for evaluation. The performance of all three injectors was found to be comparable; however, significantly different heat transfer characteristics were observed for the three injector candidates.

Typical heat flux profiles for the three candidate injectors, based on three circumferential measurements (120 degrees apart) at each axial station, are shown in Fig. 24. Although the heat flux measurements (processed to h_g measurements) were found to be approximately the same for all injectors (peak H_g about 8.5 to 10) a wide scatter in recorded heat flux was noted for the two unlike impinging injector types (Fig. 24), while that for the self-impinging doublet design showed little variation with circumferential position. These heat flux characteristics indicated that control of

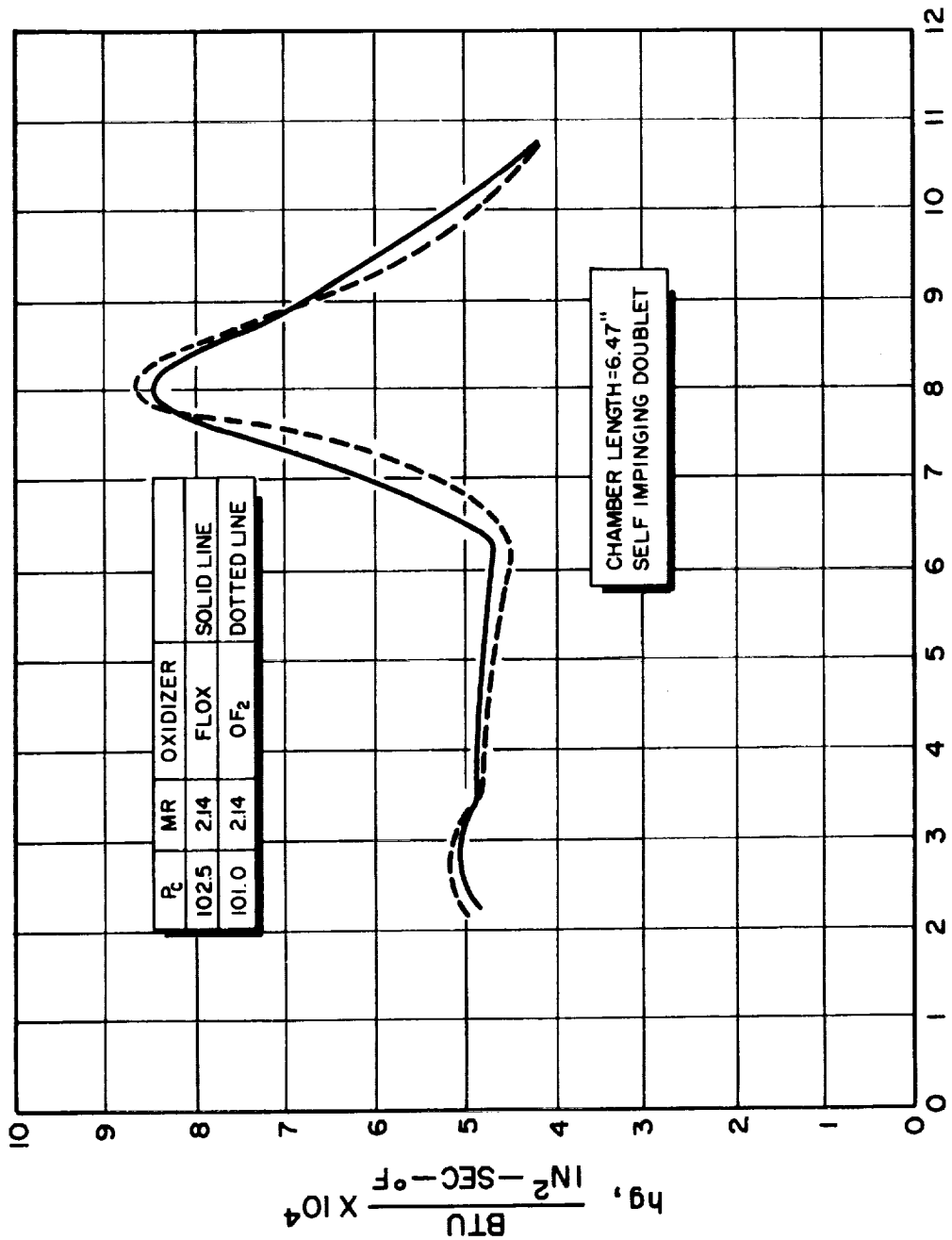

Figure 23. Comparison of Film Coefficients Realized With the Self-Impinging Doublet Injector Using FLOX/MMH and OF_2/MMH

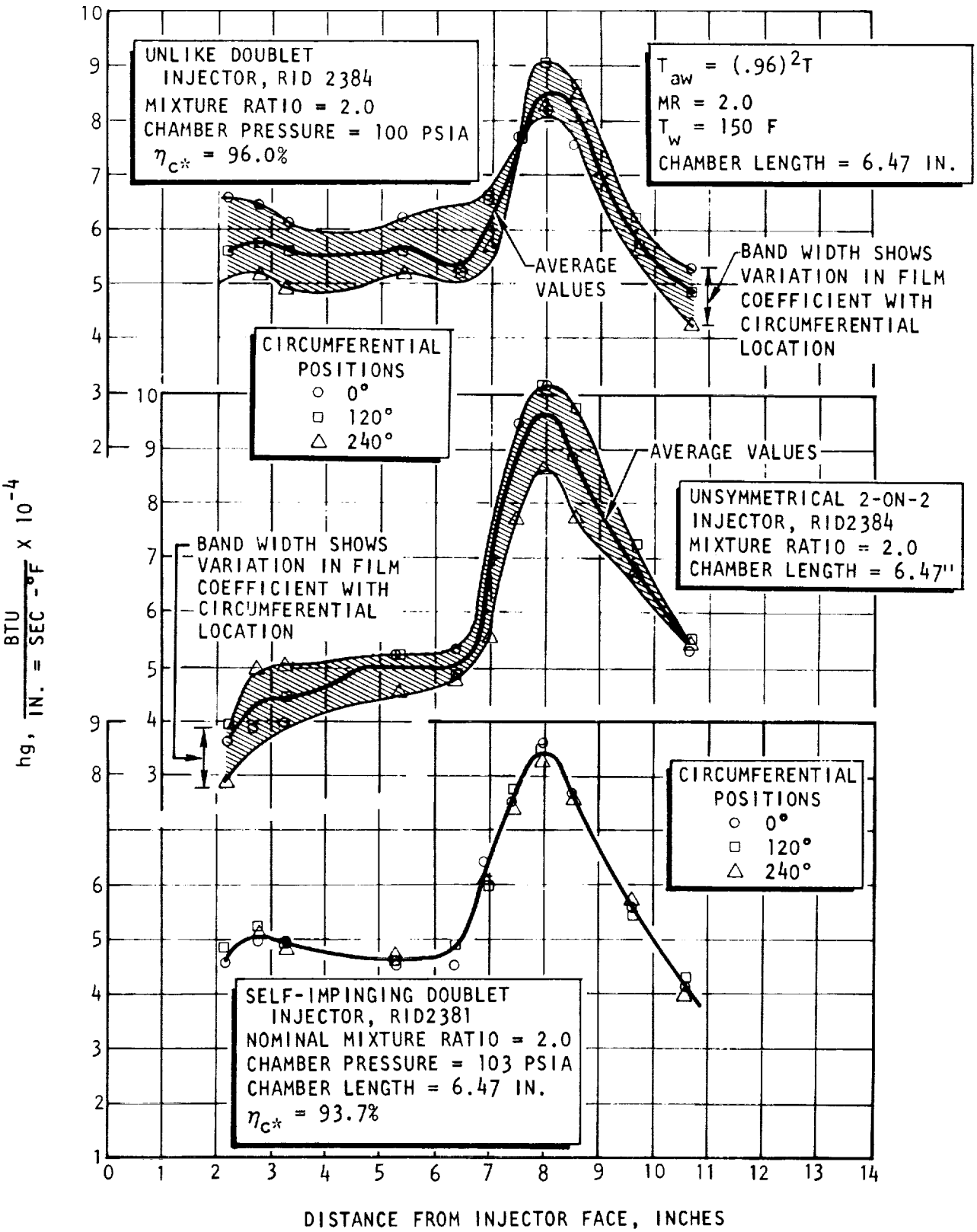

Figure 24. Chamber Heat Flux Profile for the Three Candidate Injector Patterns

propellant distribution uniformity and resultant heat transfer would be much more positive with the self-impinging design. Since the performance was comparable for all three injectors, the selection of a candidate injector type for further study was based primarily on the indicated heat transfer characteristics. Because of the apparent uniformity of the heat flux distribution, the self-impinging doublet design was selected as the prime injector type for subsequent studies.

CHAMBER CHEMICAL COMPATIBILITY

With OF_2 and the candidate space-storable fuels, C_4H_8, MMH, and B_2H_6, the primary chemical species is HF and either oxides or fluorides of the principle fuel constituent. Principle chemical species for each propellant system are shown in Table 10. For application to metallic regeneratively cooled thrust chambers, the principle species are normally considered neutral with respect to chemical attack, particularly when the gas-side wall temperature can be kept to relatively low values (1000 to 1500 F). However, for application to passively or ablatively cooled thrust chambers operating at equilibrium conditions, the interaction between the thrust chamber material and specific chemical species is of critical concern. With hydrogen-containing fuels the potential for water formation always exists. Water formation, particularly at high temperatures, would be harmful to carbon base thrust chambers, one of the few basic materials otherwise compatible with fluorine and hydrogen fluoride. The classic water-gas reaction:

$$2H_2O + C \rightarrow CO_2 + 2H_2$$

would normally preclude serious consideration of carbon and graphite materials for thrust chamber usage if the water vapor concentration were of significant magnitude. For the diborane fuel, B_2H_6, the potential for B_2O_3 formation and reaction with carbon was also of concern. The B_2O_3 species is not theoretically predicted from equilibrium considerations; however BOF, BO, and HBO all condense to B_2O_3 on the relatively cold thrust chamber wall.

TABLE 10

COMBUSTION GAS SPECIES AT CHAMBER THROAT

Species	OF_2/C_4H_8 at 3.85 mixture ratio	OF_2/MMH at 2.5 mixture ratio	OF_2/B_2H_6 at 3.87 mixture ratio
HF	47.91	50.52	32.86
CO	41.12	16.15	-
F	10.35	-	-
N_2	-	16.72	-
BOF	-	-	48.12
BO	-	-	7.12
	99.38 Percent	83.39 Percent	88.10 Percent

Residual Products

OF_2/C_4H_8: H, O, H_2, and CF (0.62 Percent)

OF_2/MMH: H, O, F, H_2, N, OH, H_2O, CO_2, NO, and O_2 (16.61 Percent)

OF_2/B_2H_6: H, O, F, H_2, OH, H_2O, O_2, B, HBO, HBO_2, BF, BF_2, and BF_3 (11.90 Percent)

With B_2O_3 and carbon at high temperature, the reaction may proceed thusly:

$$2\ B_2O_3 + 7C \rightarrow B_4C + 6CO_{gas}$$

another potentially serious impediment to carbon chamber usage.

With potential for chemical reaction with the graphite chambers, immediate concern was directed toward experimental evaluation of chamber compatibility with the carbon material. Early tests with OF_2 and FLOX/MMH at mixture ratios predicting 0.5-percent water disclosed no adverse chemical reaction of the water with the chamber material. The encouraging findings of these

early tests prompted immediate investigation into the use of passively cooled chambers with the space-storable propellants. Following design improvements on the injector and thrust chamber, tests were conducted to demonstrate that both passive and ablative thrust chambers could be designed for almost indefinite duration with OF_2/MMH at a chamber pressure of 100 psia and mixture ratio equal to 2.0, o/f.

With the OF_2/B_2H_6 combination, considerable difficulty has been encountered in maintaining minimal erosion of the throat. Although deliberate mixture ratio stratification techniques were designed into the injector for control of the peripheral temperature and chemical species, significant chamber erosion was consistently encountered with OF_2/B_2H_6. Deliberate attempts at reduction of the effective adiabatic wall temperature by lowering the peripheral mixture ratio did provide some attenuation of the apparent thrust chamber throat erosion. Use of high-strength, high-density graphite throat inserts also improved the throat erosion characteristics.

Although a strong possibility existed for chemical reaction with the carbonaceous wall material, other phenomenon observed during these experiments tend to cloud the analysis. Posttest examination of the injector face consistently resulted in observed deposition of B_2O_3 over and about the injector orifices, particularly near the outer periphery of the injector face. Although the effect of injector face deposition was not reflected in noticeable performance degradation, the extent of deposition could have seriously degraded the deliberate attempt to precisely control the propellant distribution around the thrust chamber wall. Loss of injector distribution control resulting from orifice interference could result in significant disturbance of both temperature and gas species control near the chamber wall. Because the effect of B_2O_3 deposition cannot be directly determined, some difficulty is encountered in ascertaining the exact results of this phenomena. An organized search for other candidate materials was considered, but a thorough screening study could not be accomplished within the planned scope of this program.

REGENERATIVE COOLING

Early studies during fuel selection analysis for the hydrazine-type propellants indicated that monomethylhydrazine could be used for partial regenerative cooling, even at low thrust (1000 lbf). A feasible low thrust system was one consisting of an ablative combustion chamber, a nickel, regeneratively cooled throat section, and an ablative or radiation cooled skirt. A regeneratively cooled throat section consisting of a spirally wound coolant passage and filter block was designed for experimental evaluation. A cutaway view of the basic regeneratively cooled nozzle is shown in Fig. 25. Selection of the single-pass, spiral design was dictated by the fuel flowrate limitation, particularly at the low thrust level. Design data for the nozzle were obtained from preceeding short-duration tests with uncooled copper calorimeter chambers. Convective heat transfer coefficients calculated from these data were directly applied to the design of the nozzle. A schematic of the regeneratively cooled nozzle in combination with the chamber and skirt is shown in Fig. 26.

Firings up to 600 seconds duration were conducted; however, initial experimentation resulted in random nozzle failures, particularly near the start of convergence to the throat. Detailed analysis of the prevailing nozzle heat load disclosed a substantial heat load contribution due to radiation from the hot ablative chamber sections fore and aft of the regenerative nozzle. It was found that the added local heat load at the start of convergence was approximately 50 percent higher than that estimated from the short-duration tests conducted with the all-copper thrust chamber. Appropriate increase in heat transfer capability was incorporated into the nozzle design by reducing the coolant passage area in this critical region and subsequent tests were found to be completely satisfactory.

The results of one of the tests are shown in Fig. 27. Here, the analytical predictions for the nozzle heat load are based on both the direct convective load and the additional contribution due to radiation from the hot chamber wall. The actual experimental measurements taken during a long-duration

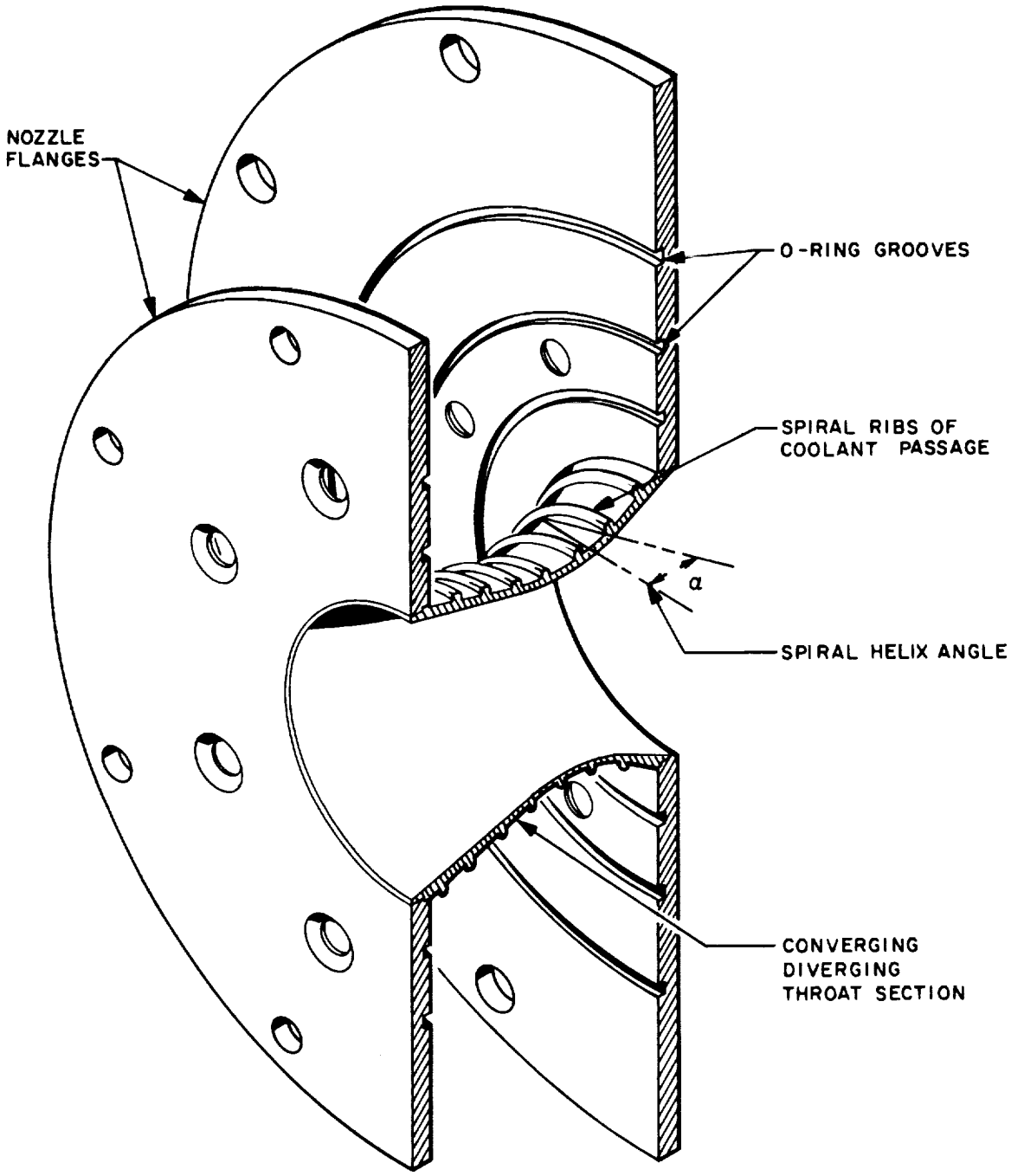

Figure 25. Cutaway View of Regeneratively Cooled Nozzle Showing General Design Features Applicable to Nickel-A Nozzles No. 3 and 4

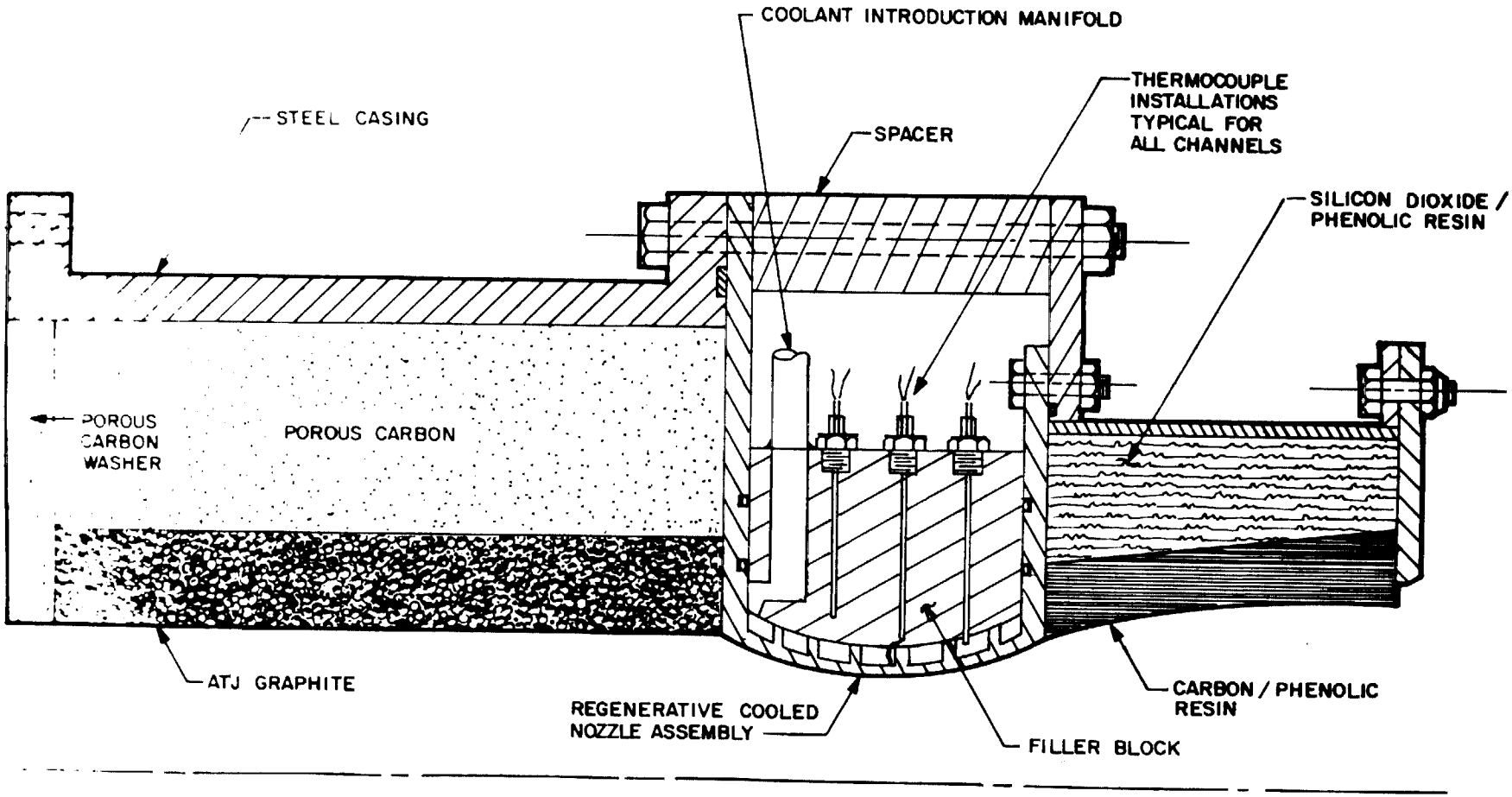

Figure 26. Cross-Sectional View of Ablative Thrust Chamber Assembly Used in Multiple Restart and Chamber Pressure/Mixture Ratio Excursion Firings

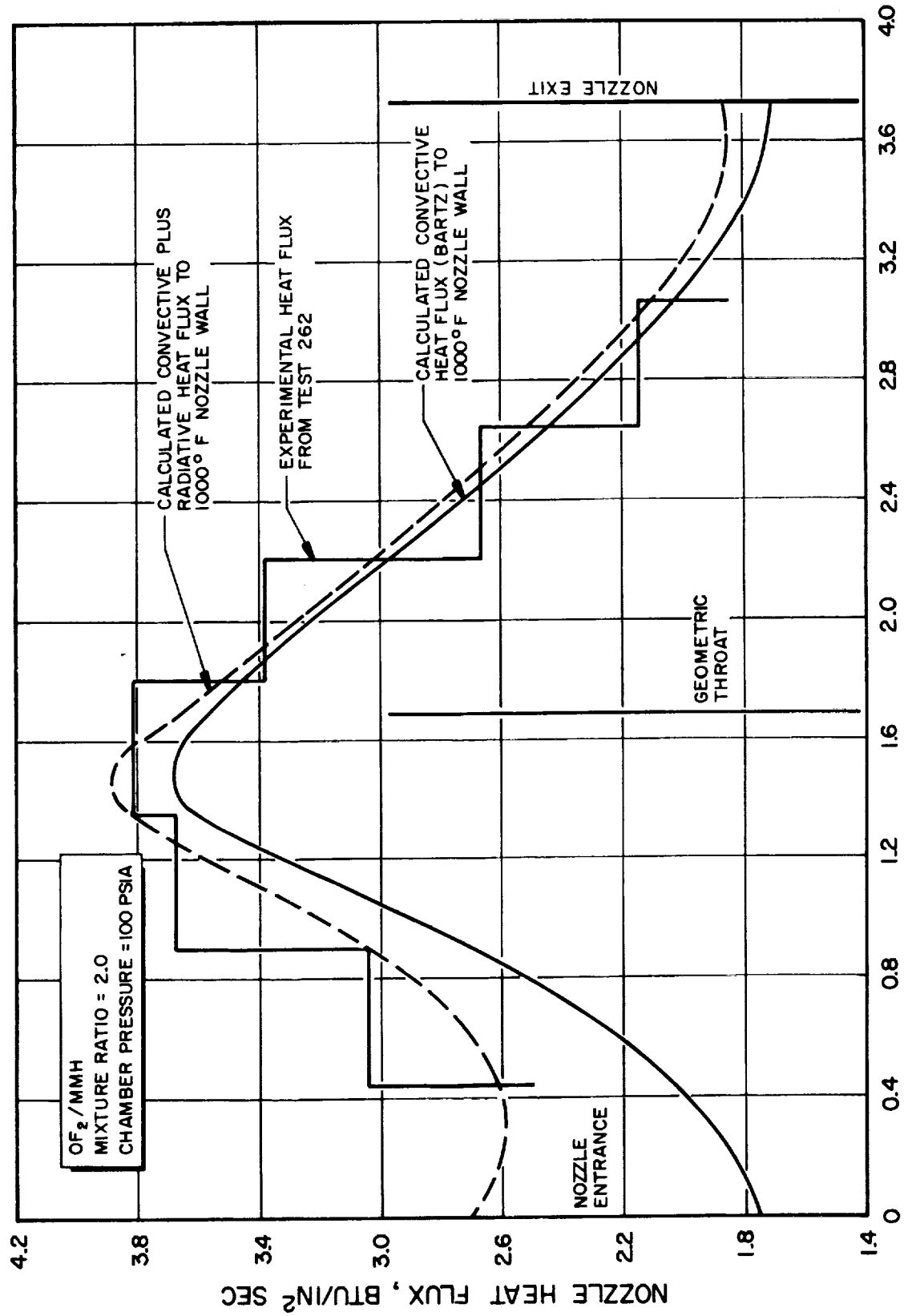

Figure 27. Comparison of Theoretically Predicted Heat Flux and Experimentally Determined Heat Flux From Typical Test With Regeneratively Cooled Nozzle

test are also shown as steps on Fig. 27. The close correspondence between analysis and experiment tends to confirm the validity of the heat transfer analysis.

In addition to basic nozzle evaluation, additional studies were conducted to determine the limits of operation in a regenerative mode. Test firings were conducted at nonoptimum conditions to define a suitable operating envelope for regenerative cooling.

A series of tests conducted at various chamber pressures and mixture ratios indicated that operation at 180-psia chamber pressure and a mixture ratio of 2.5 was not feasible for regenerative operation. On the other hand, reducing chamber pressure and mixture ratio to 50 psia and 1.5, respectively, was completely satisfactory for regenerative operation. The results of this test series plainly indicated that probability for nozzle failure was greatest with increasing chamber pressure and mixture ratio.

Concluding tests were conducted to demonstrate multiple restart capability for the regeneratively cooled OF_2/MMH thrust chamber. At nominal design operating conditions, one experiment was conducted in which nine starts of 10 seconds each with "off-times" increasing geometrically from 2 to 18 seconds. The MMH was supplied first to the nozzle cooling passages and then to the injector in a full regenerative mode. No failures or evidence of fuel decomposition occurred at any time during this test. This final experiment verified that the existing nozzle design was satisfactory under conditions closer to that which might be encountered in actual manuever operations. In general, multiple restart capability was fully demonstrated in this single test. It is probable, however, that a positive cooling system vent would be required for a practical engine because of the anticipated high temperature which will be encountered due to thermal soakback from the passively cooled chamber components during long shutdown periods.

ABLATIVE COOLING

Alternate nozzle design concepts using passive cooling techniques were also investigated to provide design technology for eventual replacement of the

regeneratively cooled nozzle section. The results of early exploratory tests using ATJ-graphite throat inserts combined with carbon-base ablative thrust chambers indicated a promising potential for successful application to the OF_2/MMH system. Design criteria were then generated for promotion of low overall char rate and to long-duration surface stability, particularly in the throat region.

With respect to the combustion chamber itself, studies were conducted to determine the effect of cloth laminate orientations and structural geometry on char characteristics and, also, briefly, the effect of the resin content within the carbon fiber reinforcing matrix. The effects of film angle orientation and resin content were conducted with composite thrust chambers having the cylindrical combustion chamber sections made up with various laminate angle orientation, ranging from 6- to 90-degrees to the chamber centerline. The results of testing clearly indicated that char rate was strongly dependent on the cloth laminate angle and that the cylindrical chamber section consisting of 6-degree cloth orientation exhibited the lowest overall char rate. In fact, the experimental char rate was found to compare quite favorably with that previously reported for refrasil/phenolic, a well-established insulating ablative. The results of this test series gave positive indication that the ablative chamber section should consist of near-parallel wrapped laminates. A fully parallel orientation was expected to provide some difficulty with respect to surface delamination. It was also found during this test series that the amount of resin content had little effect on overall char; however, its effect on the strength of the resulting charred matrix was not ascertained.

With respect to structural design, subsequent experiments clearly indicated that composites with uninterrupted axial conduction paths definitely resulted in a more uniform char profile. A relatively flat and uniform char profile would be favored for reduction of the overall weight of the thrust chamber.

Based on these experiments, sufficient design criteria were established for confident design of improved thrust chambers for long-duration evaluation. Chambers such as shown in Fig. 28 were fabricated and tested with FLOX/MMH

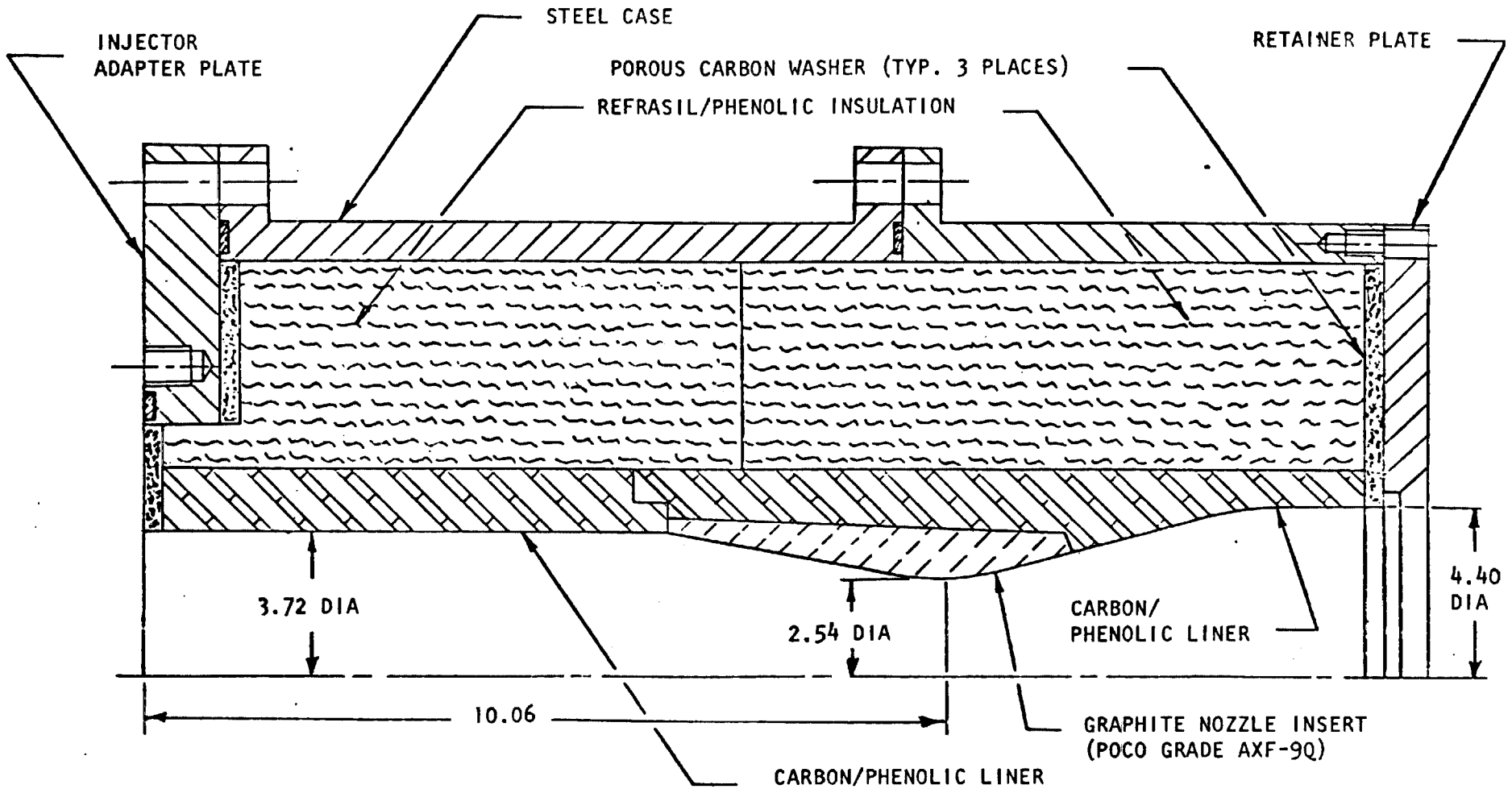

Figure 28. Schematic Cross Section of Typical Long Duration Chamber Assembly

and run for as long as 1000 seconds with little or no measureable throat or chamber erosion. Further improvements in material and fabricating techniques permitted design of a flight-type lightweight thrust chamber for FLOX/MMH at elevated chamber pressures. This lightweight, high-pressure thrust chamber is shown in Fig. 29. One test at 500 psia was conducted for 150 seconds with FLOX/MMH with virtually no throat erosion. Additional tests at the nominal 100 psia condition were also conducted with FLOX/butene-1 with similar satisfactory results. These same basic chamber design criteria were then also extended to the high energy OF/B_2H_6 propellant combination. Tests up to 150 seconds duration were satisfactorily conducted with only moderate throat erosion; however, one attempt at extending the practical duration to 370 seconds resulted in severe thermochemical erosion of both chamber and throat. Even with selection of improved high density graphite throat inserts, significant erosion was experienced with the carbon base thrust chambers when using OF_2/B_2H_6. Two potential reasons can be hypothesized; (1) that gradual deposition of combustion products in the injector face eventually degrades the deliberate attempt to control the gas environment at the chamber wall, and (2) that carbon base material are subject to chemical attack by harmful combustion product species.

INTEREGEN COOLING

Concluding program tasks were directed to evaluation of the Rocketdyne developed "interegen" cooling concept for potential application to the high energy OF_2/B_2H_6 propellant combination. Initial effort was directed toward analytical determination of cooling feasibility using B_2H_6 as a film coolant on the thrust chamber wall. Thermal analyses were also conducted to select a promising thrust chamber material and configuration for a complete interegen assembly. Analytical perturbations were conducted to assess injector design effects on the overall performance when a portion of the fuel is employed as a film coolant. Estimates were made of the prevailing adiabatic wall temperatures and approximate temperature profile determinations were made for various thrust chamber materials and geometries. These studies clearly indicated that B_2H_6 film cooling could be effected without severe performance degradation.

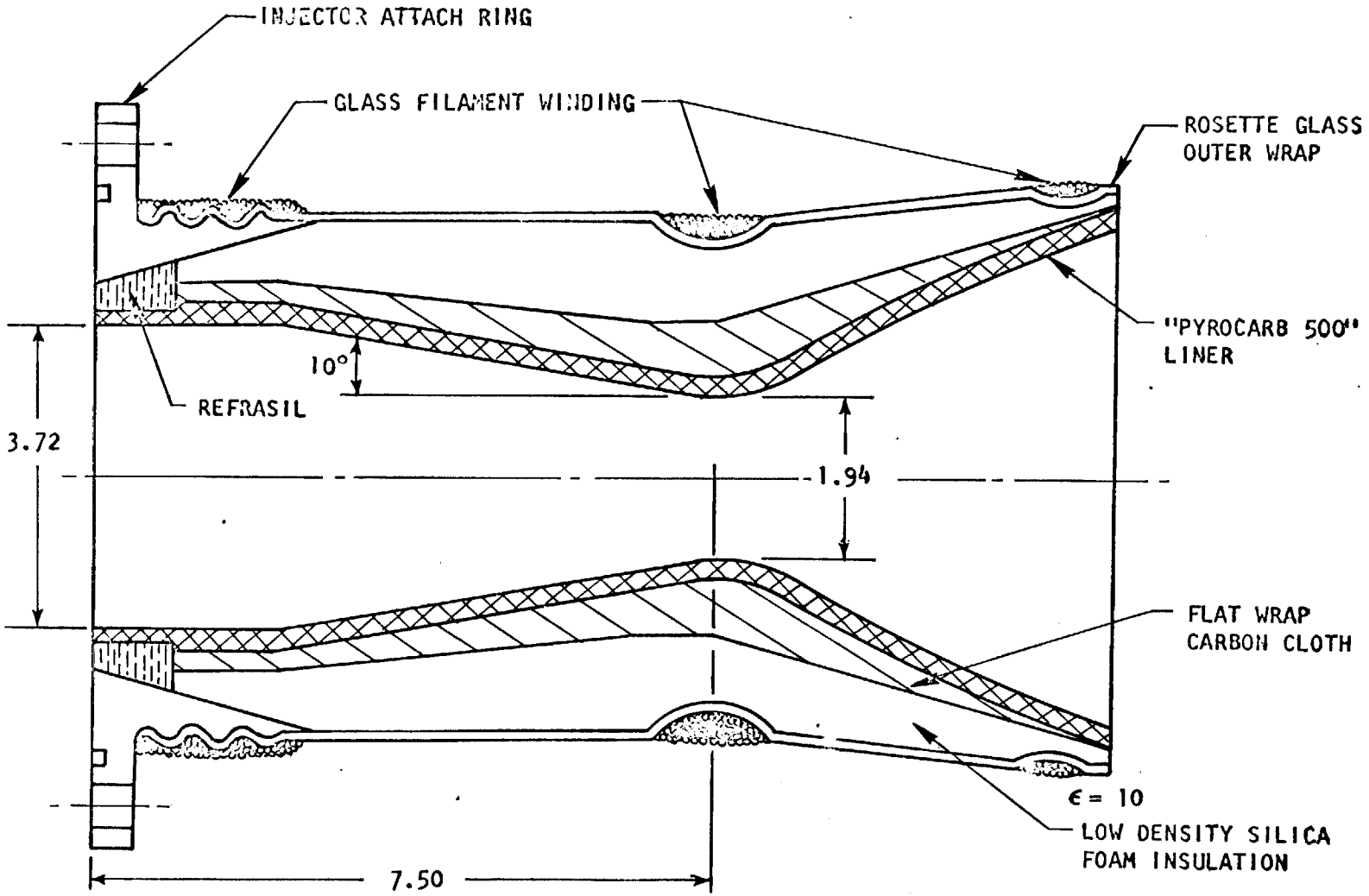

Figure 29. Lightweight Passive Thrust Chamber for High-Pressure Operation With FLOX/MMH

Short duration experiments were conducted with both copper and graphite thrust chambers to evaluate injector performance and heat transfer characteristics. The injector best suited for high performance and material compatibility with the cooling scheme was determined to be similar in design to the basic self impinging doublet injectors previously used throughout the program. The specific design for peripheral injection of B_2H_6 film coolant was found to be an outer ring which provided a tangential swirl to the film coolant. A complete injector was fabricated and extensive short duration tests were conducted in copper calorimeter thrust chambers to assess effects of both core and film coolant injection characteristics on performance and heat transfer. A single test of the complete interegen thrust chamber assembly was conducted to determine the practical feasibility of this cooling concept. Target test conditions were 100-psia chamber pressure, a mixture ratio of 3.0 for the injector core, and 10-percent fuel film coolant. The test was programmed for over 300 seconds of operation but was prematurely terminated after 45 seconds because of chamber structural failure.

Posttest analysis disclosed that the most probable mode of failure was the superposition of high local thermal stresses resulting from injector oxidizer misimpingement, with the normal chamber thermal stresses and to clamp ring loads. Analysis had disclosed that the graphite chamber could have run to thermal equilibrium with reasonable throat temperatures; however, high stresses would have eventually occurred because of the method of injector to chamber attachment.

It was also apparent from the results of this test that appropriate design criteria will require longer duration tests in appropriately designed thrust chambers to more fully define the interior driving temperature and the film coolant heat transfer characteristics. The test results also clearly indicate that control of combustion product deposition and nozzle erosion are also essential for eventual development of a fully satisfactory OF_2/B_2H_6 interegen thrust chamber assembly. Test of the complete injector with film coolant showed that the injection of 10 percent of the total

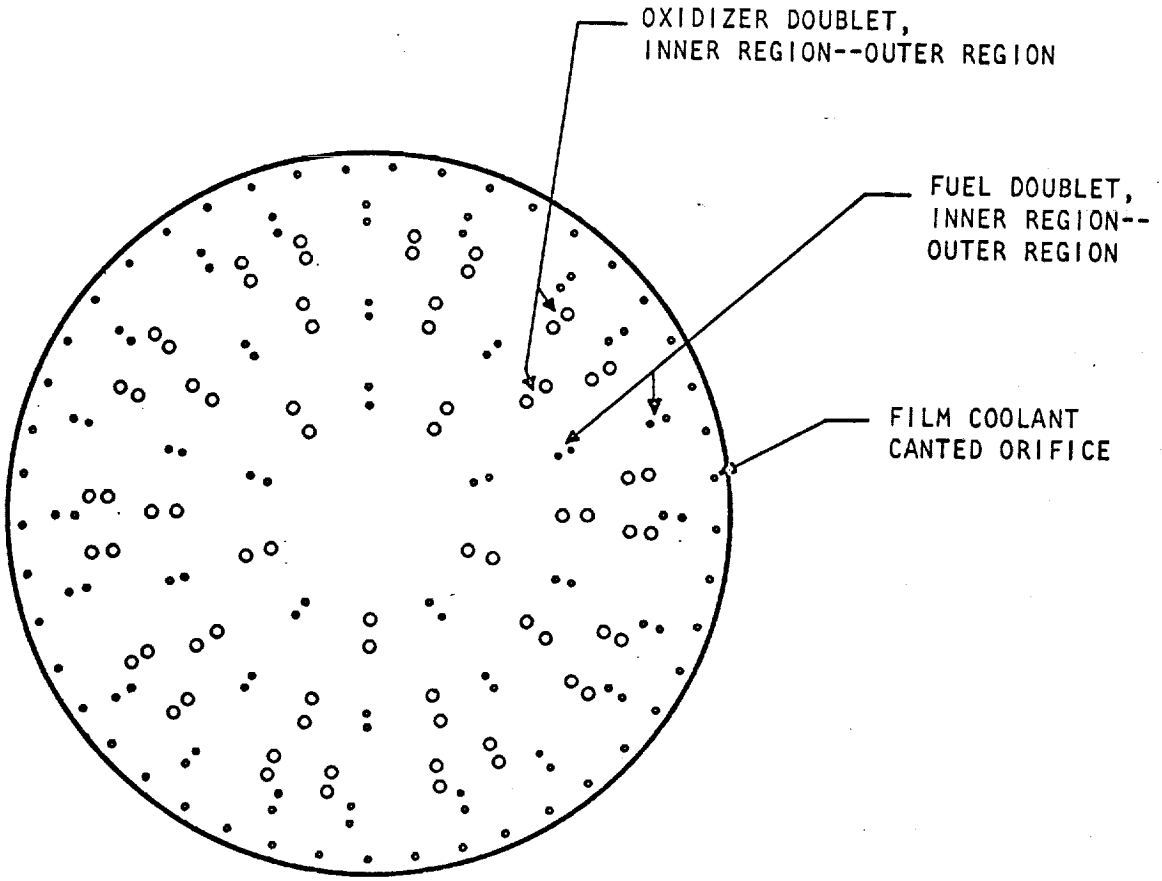

INJECTOR ZONE: PHYSICAL DESCRIPTION	INNER REGION: LIKE DOUBLET, ALIGNED OXIDIZER AND FUEL FANS	OUTER REGION: LIKE DOUBLET, OFFSET OXIDIZER AND FUEL FANS	FILM COOLANT: SINGLE ORIFICE, CANTED 25 DEGREES TOWARD WALL
NOMINAL MIXTURE RATIO (O/F)	3.85	3.25	0.0
MASS DISTRIBUTION	70 PERCENT OF CORE FLOW	30 PERCENT OF CORE FLOW	VARIABLE PERCENTAGE OF TOTAL FLOW
OXIDIZER ORIFICE DIAMETER, INCH	0.036	0.020	--
FUEL ORIFICE DIAMETER, INCH	0.024	0.0145	0.018
NOMINAL ORIFICE PRESSURE DROP, PSI	100	100	20 TO 100

Figure 30. Modified Interegen Injector Face Pattern (2768) and Propellant Distribution Characteristics

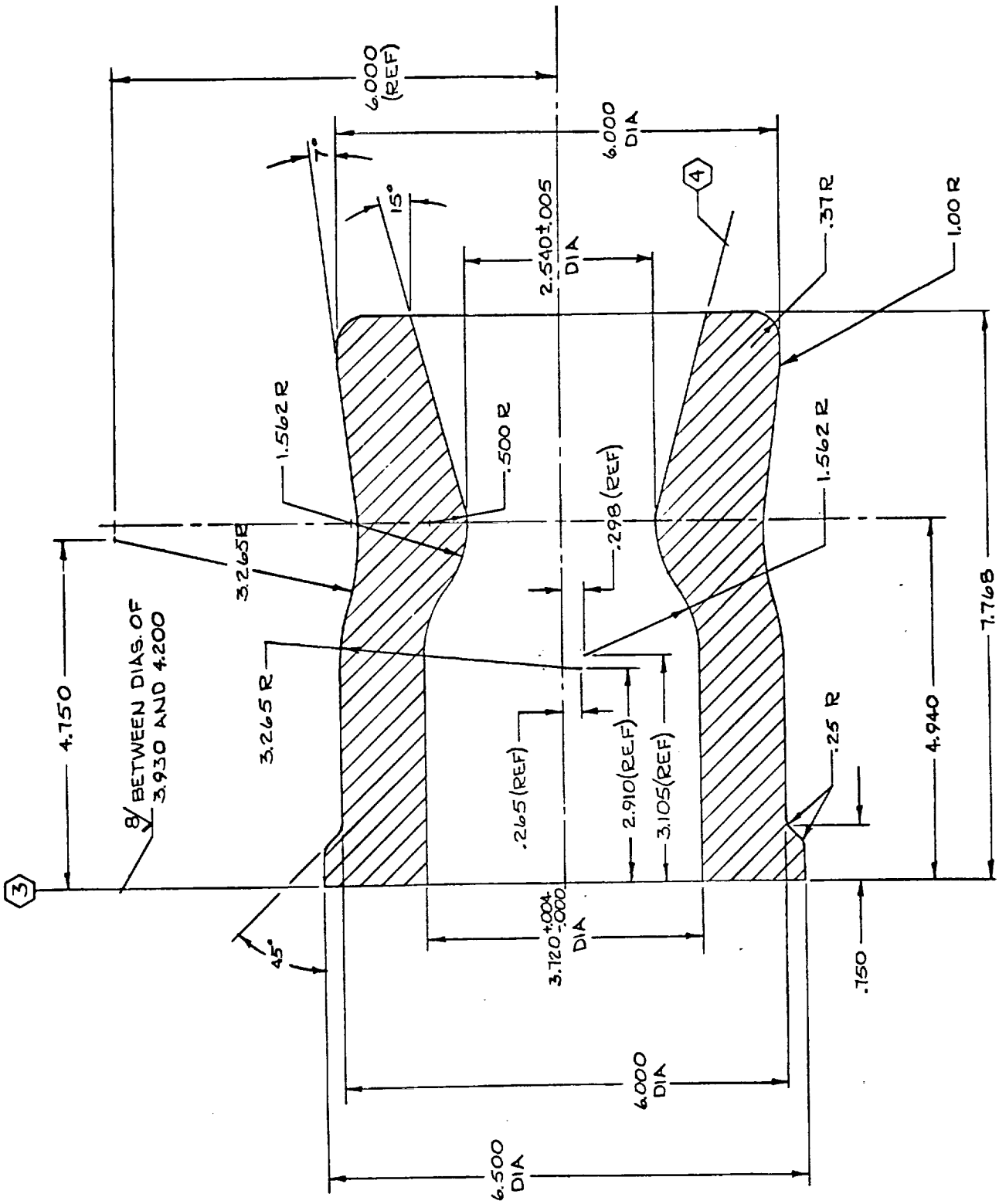

Figure 31. Interegen Graphite Thrust Chamber

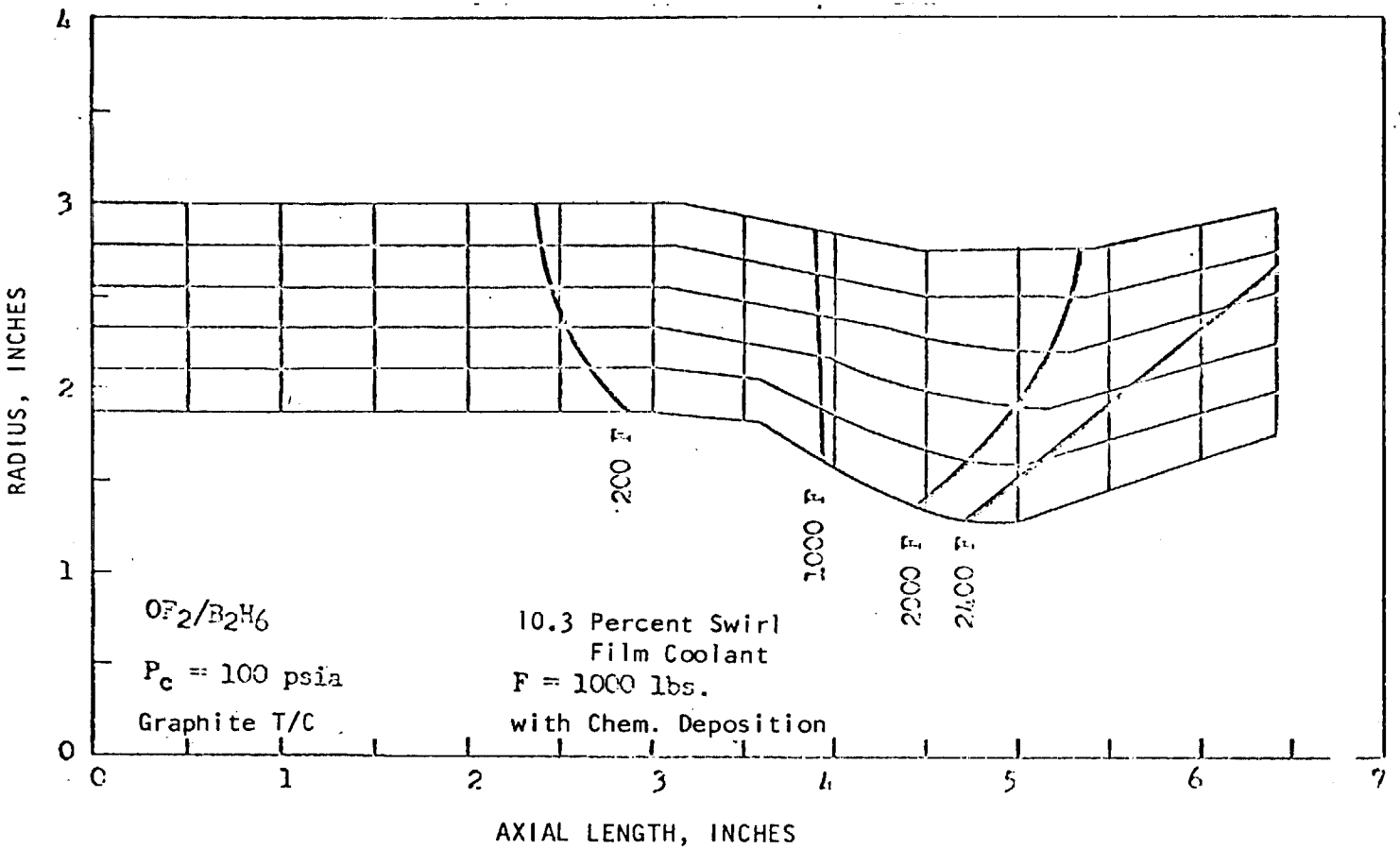

Figure 32. Predicted Thrust Chamber Isotherms at 400 Seconds of Sustained Operation

propellants as B_2H_6 film coolant could be accomplished without severe performance penalties. High cooling efficiencies were observed at these injection conditions. A schematic of the final basic injector design is shown in Fig. 30. The swirl coolant ring is illustrated in Fig. 86 of Ref. 4.

The performance and heat transfer data were used to modify the assumptions made in preliminary determination of operational feasibility. The thermal analysis model was re-evaluated with the newly developed empirical data and a final assessment of the prevailing thermal conditions was made. In additon, a stress analysis was also conducted to assess both transient and steady state loads for typical chamber materials and configurations. A high strength graphite (POCO AXM) was selected for the thrust chamber because of its favorable thermal and strength characteristics. Using this material a single thrust chamber design was selected for fabrication and testing. A schematic of the one-piece thrust chamber assembly is shown in Fig. 31.

The anticipated temperature isotherms for this chamber at the conclusion of 400 seconds of operation are shown in Fig. 32. As may be noted from this model prediction, maximum temperatures less than 3000 F were anticipated, which is well within the practical operating range for graphite.

CONCLUSIONS

The results of this 5-year applied research program have provided valuable design criteria for several selected space storable propellants featuring oxygen-difluoride (OF_2). Although not fully developed for OF_2/C_4H_8 and OF_2/B_2H_6, the design criteria generated for OF_2/MMH is sufficient to proceed into early development of an advanced space propulsion system. Insufficient criteria for thrust chamber cooling would restrict the immediate application of the other candidate space storable systems.

The analytical technique used for selection of candidate space storable fuels is a rational method for preliminary propellant definition. Although an optimum fuel cannot be generally defined, the division of selection criteria to payload and performance, operational aspects, and cooling capability does enable the system analyst to define those criteria most important to the specific mission and to weigh the selection accordingly. However, based on satisfaction of broad rating categories, it was found that MMH, C_4H_8, and B_2H_6 were optimum choices within their respective fuel categories.

Design criteria were generated and experimentally demonstrated for high performance with all three propellant combinations. Moreover, it was shown that basic physical principles could be used to accurately predict the behavior of each propellant system. It was also shown that c* performance is dictated only by the combined effect of propellant mixing and vaporization. In general, high delivered performance could be predictably delivered with any of these candidate propellant systems.

Simulated altitude tests clearly demonstrated that nozzle efficiencies could also be analytically predicted. Experiments proved that 10:1 throttling could be effected for all of the propellants with acceptably high efficiency.

It was conclusively demonstrated that heat transfer characteristics for each of the propellant systems could be controlled through injector design. OF_2/MMH was fired successfully in both regenerative and ablative thrust chambers. Although long-duration capability has not been fully demonstrated with OF_2/C_4H_8 and OF_2/B_2H_6, valuable experimental data has been developed for eventual acquisition of this technology.

REFERENCES

1. Lambiris, S., L. P. Combs, and Levine R. S., "Stable Combustion Processes in Liquid Propellant Rocket Engines," Combustion and Propulsion, Fifth AGARD Colloquium: High Temperature Phenomena, The MacMillan Company, New York, N. Y., 1962.

2. Ingebo, R. E., Dropsize Distributions For Impinging-Jet Backup in Airstreams Simulating the Velocity Condition in Rocket Combustors, NACA TN 4222, 1958.

3. Rupe, J. H., The Liquid Phase Mixing of a Pair of Impinging Streams, JPL PR20-195, Jet Propulsion Laboratory, Pasadena, California, 1953.

4. R-7985, Chamber Technology for Space Storable Propellants, Fourth Interim, Rocketdyne, a Division of North American Rockwell Corporation, Canoga Park, California, September 1969.

UNCLASSIFIED

Security Classification

DOCUMENT CONTROL DATA - R & D

(Security classification of title, body of abstract and indexing annotation must be entered when the overall report is classified)

1 ORIGINATING ACTIVITY (Corporate author) Rocketdyne, a Division of North American Rockwell Corporation, 6633 Canoga Avenue, Canoga Park, California 91304	2a. REPORT SECURITY CLASSIFICATION UNCLASSIFIED 2b. GROUP 4

3 REPORT TITLE

CHAMBER TECHNOLOGY FOR SPACE STORABLE PROPELLANTS

4 DESCRIPTIVE NOTES (Type of report and inclusive dates)

Final Report, June 1964 through September 1969

5 AUTHOR(S) (First name, middle initial, last name)

6 REPORT DATE 6 March 1970	7a. TOTAL NO. OF PAGES 116	7b. NO. OF REFS 4
8a. CONTRACT OR GRANT NO. NAS7-304 b. PROJECT NO. c. d.	9a. ORIGINATOR'S REPORT NUMBER(S) R-7998 9b. OTHER REPORT NO(S) (Any other numbers that may be assigned this report)	

10 DISTRIBUTION STATEMENT

This material contains information affecting the National Defense of the United States within the measning of the Espionage Laws, Title 18 U.S.C., Sections 793 and 794, the transmission or revelation of which in any manner to an unauthorized person is prohibited by law.

11 SUPPLEMENTARY NOTES	12. SPONSORING MILITARY ACTIVITY NASA

13 ABSTRACT

A 5-year applied research program has been conducted to generate chamber technology for several space storable propellant combinations featuring oxygen difluoride (OF_2) oxidizer. The fuels evaluated for combination with OF_2 were monomethylhydrazine (MMH), butene-1 (C_4H_8) and diborane (B_2H_6). Extensive design criteria were developed for OF_2/B_2H_6 and OF_2/C_4H_8. A full analysis technique was developed for rational selection of optimum fuels for combination with OF_2. Selection of the candidate fuels was based on performance, operational aspects, and compatibility for thrust chamber cooling. Areas of investigation included injector performance, performance demonstration under simulated altitude conditions for OF_2/MMH, and throttling characteristics for all of the propellant combinations. Complete assessment of heat transfer characteristics were conducted for each propellant system. Design criteria were generated for either regenerative or ablative cooling with OF_2/MMH. Passive cooling technology was also developed for OF_2/B_2H_6; however, the OF_2/C_4H_8 studies were limited to heat transfer characterization.

DD FORM 1 NOV 65 1473

UNCLASSIFIED

Security Classification

14 KEY WORDS	LINK A		LINK B		LINK C	
	ROLE	WT	ROLE	WT	ROLE	WT
Space Storable Propellant Combinations						
Oxygen Difluoride (OF_2) Oxidizer						
Candidate Fuels						
OF_2/MMH						
OF_2/B_2H_6						
OF_2/C_4H_8						